Modeling Engineered Nanoparticles Removal by Conventional Activated Sludge Treatment Process in Wastewater Treatment Plant

by

Zhicheng Yu

A Thesis Presented in Partial Fulfillment
of the Requirements for the Degree
Master of Science

Approved April 2015 by the
Graduate Supervisory Committee:

Paul Westerhoff, Chair
Bruce Rittmann
Pierre Herckes

ARIZONA STATE UNIVERSITY

May 2015

ABSTRACT

The production and applications of engineered nanomaterials (ENM) has increased rapidly in the last decade, with release of ENM to the environment through the sewer system and municipal wastewater treatment plants (WWTPs) being of concern. Currently, the literature on ENM release from WWTPs and removal of ENM by WWTPs is insufficient and disorganized. There is little quantitative data on the removal of multi-walled carbon nanotubes (MWCNTs), graphene oxide (GO), or few-layer graphene (FLG), from wastewater onto biomass. The removal of pristine and oxidized MWCNTs (O-MWCNTs), graphene oxide (GO), few-layer graphene (FLG) and Tween™ 20-coated Ag ENM by the interaction with biomass were determined by programmable thermal analysis (PTA) and UV-Vis spectrophotometry. The removal of pristine and O-MWCNTs was 96% from the water phase via aggregation and 30-min settling in presence or absence of biomass with an initial MWCNT concentration of 25 mg/L. The removal of 25 mg/L GO was 65% with biomass concentration at or above 1,000 mg TSS/L. The removal of 1 mg/L FLG was 16% with 50 mg TSS/L. The removal of Tween™ 20 Ag ENM with concentration from 0.97 mg/L to 2.6 mg/L was from 11% to 92% with biomass concentration of 500 mg TSS/L to 3,000 mg TSS/L, respectively.

A database of ENM removal by biomass was established by analyzing data from published papers, and non-linear solid-liquid distribution functions were built into the database. A conventional activated sludge (CAS) model was built based on a membrane bioreactor (MBR) model from a previous paper. An iterative numeric approach was adapted to the CAS model to calculate the result of non-linear adsorption of ENM by biomass in the CAS process. Kinetic studies of the CAS model showed the model

performance changed mostly in the first 10 days after changing influent chemical oxygen demand (COD) concentration, and reached a steady state after 11 days. Over 60% of ENMs which have distribution coefficients in the database reached higher than 50% removal by the CAS model under general operational conditions. This result suggests that traditional WWTP which include the CAS process can remove many known types of ENMs in certain degree.

DEDICATION

I dedicate this thesis to those who have loved me and supported me through this chapter of my life. Especially, my beloved family has always been the source of power for me to conquer all obstacles. Although thousands miles away from home across the Pacific Ocean, I did not feel alone in the Sonoran desert. Wherever I will be in the future, I will always treasure the friendship, love, memories of joy and tears in here, in the white sand and red dirt of Arizona.

ACKNOWLEDGMENTS

I would like to thank my committee for their trust and guidance throughout my research. I would like to express my deepest gratitude to my advisor, Dr. Paul Westerhoff for offering me this precious opportunity to pursue my Masters Degree. You have guided me with vast knowledge and insights for research. I would like to thank my other committee members, Dr. Bruce Rittmann and Dr. Pierre Herckes for offering me advice and support through these two years. I would like to thank Dr. Kiril Hristovski for all the advice on Friday meetings. I'm also grateful to all fellow researchers of our lab, Dr. Onur Apul, Dr. Robert Reed, Dr. Ting Lei, Xiangyu Bi, Natalia Fischer, Mac Gifford, David Hanigan, Heuidae Lee, Dylan Lesan, Marisa Masles, Anjali Mulchandani, Natalia von Reitzenstein, Jared Schoepf, Heather Stancl, for providing such friendly and passionate atmosphere that light up the time of my research life. I would like to give an extra thank you to Dr. Yu Yang, who offered me great help in my research experiments.

I would like to thank United States Environmental Protection Agency (USEPA) and National Science Foundation (NSF) for providing the funding of this research.

TABLE OF CONTENTS

Page

CHAPTER Page

LIST OF TABLES

LIST OF FIGURES

Figure Page

Figure Page

CHAPTER 1

OVERVIEW

1.1 Introduction

Nanotechnology has developed over the last decade and lead to breakthroughs in several industrial fields which include foods, electronics, paints, textiles, catalytic, pharmaceuticals and cosmetics (Bystrzejewska-Piotrowska, Golimowski et al. 2009, Bhatt and Tripathi 2011). The term nano derives from the Greek word *nanos* which means a dwarf. The definition of nanomaterials (NMs) is the length of the material is less than 100 nm in at least one dimension, while the definition of nanoparticles (NPs) is the material with length from 1 to 100 nm in at least two dimensions (Klaine, Alvarez et al. 2008). Natural NMs include materials such as aerosols, proteins, nucleic acids, humic and fulvic acids, virus in the atmosphere, aquatic phase and terrestrial.

Engineered nanomaterials (ENMs) have unique characteristics including large specific surface area, high surface energy, and quantum confinement. ENMs include silver (Ag), gold (Au), titanium oxide (TiO_2), silica oxide (SiO_2), cerium dioxide (CeO_2), zinc oxide (ZnO), carbon nanotubes (CNTs), graphene, graphene oxide, fullerene (C_{60}), quantum dots and others. Sources of ENMs from applications are included in Table 1. The production, manufacture and consumer usage rate of ENMs increased rapidly in this decade, which also increased the environmental release of ENMs (Mangematin and Walsh 2012, Nowack, Ranville et al. 2012).

Environmental toxicologists and biologists have raised concern about potential adverse impacts of ENMs to animals, plants, as well as to the environment (Colvin 2003, Moore 2006, Nowack and Bucheli 2007, Drobne, Jemec et al. 2009, Ma, Geisler-Lee et

al. 2010). Thus it is necessary to study the potential impact of ENMs to the environment, and quantify the release of ENMs to the environment.

Table 1. Example Applications of Different Class of ENMs

Class of ENMs	**Example Applications**
Silver Nanoparticles (AgNPs)	Toothpastes, baby products, textiles, washing machines
Gold Nanoparticles	Catalyst, vector in tumor therapy
TiO_2	Cosmetics, paints, coatings
SiO_2	Batteries, paints, adhesives, cosmetics, glass, steel, fiber, glass
CeO_2	Combustion catalyst in diesel fuels, metallurgical and glass/ceramic application
ZnO	Skin care products, bottle coatings
Carbon nanotubes (CNTs)	Electronics, plastics, sporting goods, catalysts, water purification systems as sorption material, aircrafts, aerospace
Graphene	Medicine, electronics, light processing, energy, sensors
C_{60}	Cosmetics
Quantum dots	Medicine, medical imaging, solar cells

1.2 Conventional Activated Sludge Treatment Process

In 1914, E. Ardern and W.T. Lockeet discovered the activated sludge process in England (Ardern and Lockett 1914). The activated sludge process reduced the time period to remove organic contaminants to a satisfactory level from days to hours. The typical CAS process includes aeration tank, secondary clarifier, a recycle pipeline, and a sludge wasting pipeline (Figure 1). The main interaction between microbial aggregates and contaminants take place in the aeration tank.

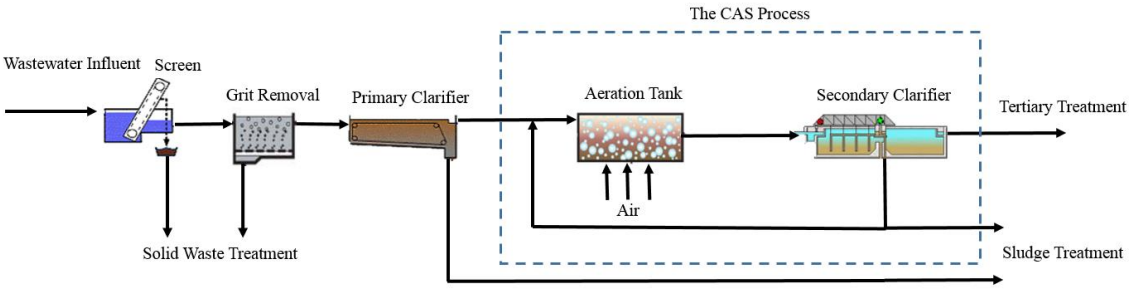

Figure 1. Typical design of the CAS Process with Primary Treatment Processes

The CAS process has become the most widely used biological processes for wastewater treatment worldwide because it is flexible, robust and cost-effective. However, during a very long period from 1914 to about 1950s, the CAS reactors were designed and operated based upon experience and rule-of-thumb. It was until 1950s that theories of operation were finally sufficient so the CAS reactors could be designed by characteristics of the influent wastewater (Monod 1950). Even though the CAS process has been widely applied worldwide and has reached large-scale success in wastewater treatment, it does not necessarily mean it is flawless. The large scale of the reactor makes it difficult to control the reactor's parameters precisely. It is also difficult to control the

composition of microorganisms in the tank, which is the key to successful treatment. The change of the composition of the microorganisms can lead to significant problems such as sludge bulking.

1.3 ENMs in Wastewater Treatment Plant (WWTP)

1.3.1 Source of ENMs in Sewage

The application of ENMs has experienced exponential growth in this decade, and there are at least four different types of product lines of ENMs that could lead to different release scenarios (Westerhoff, Kiser et al. 2013). First, dispersed ENMs are incorporated into food products, which include liquids, gels or dissolvable solids. Second, surface-attached ENMs are used in fabrics and food packaging for antibacterial purpose. Third, polymeric-embedded ENMs are added to materials as a structure or performance enhancer. Fourth, industrial processing ENMs are being used as catalysts or polishing agents during manufacturing. All ENMs from these four different product lines are possibly released directly into the sewage system during the process of manufacturing, use or disposal.

Researchers have already identified ENMs in sewage sludge of WWTP (Kim, Park et al. 2010). WWTP serves as a monitor of contaminants that are generated by all kinds of human and nature activities, thus WWTP can be a perfect observatory for ENMs.

1.3.2 Relevance of ENMs in Wastewater and Sewage Sludge

One of the major functions of the WWTP is to remove carbon, nitrogen and pathogens from wastewater. The removal of ENMs in WWTPs occurs either by design or by the removal of the other pollutants. There are two endpoints for the ENMs in the

wastewater. They can end up in the effluent from WWTP, or in the sewage sludge which ends up in land application, incineration or landfill (Brar, Verma et al. 2010). The proportion of ENMs that ended up in effluent (i.e. liquid phase) or sewage sludge (i.e. solid phase) is determined by a distribution factor that relates to sorption, aggregation, agglomeration and settlement. Aggregation, sorption and agglomeration are the dominant processes of the reactions of ENMs in WWTP. The removal of ENMs in WWTP happens mostly in primary treatment and secondary treatments.

Primary and secondary clarifiers are treatment processes that remove ENMs by sedimentation after ENMs aggregate with other particles in WWTP. The purpose of primary clarifier in WWTP is to remove suspended inorganic particles by gravity settlement. However, because of the presence of biomass in primary and secondary clarifier, association of ENMs to biomass via aggregation plays important role during the removal process. Suspension with low stability tends to aggregate over time, thus increases the particle size and decreases the concentration of the suspension by gravitational settling. For particles smaller than 300 nm, Brownian motion dominates the process of aggregation. The key factors that will affect colloidal stability include pH value, electrolyte valence, and particle coating (Stankus, Lohse et al. 2011).

During the CAS process, the nanoparticles interact with microorganisms in the aeration tank and second clarifier. The interaction includes adherence of nanoparticles to the cell surface or extracellular polymeric substance (EPS), and active or passive transport through membrane or across the cytoplasmic membrane (Kloepfer, Mielke et al. 2005). These interactions can affect the microorganisms metabolic activities and thus

change the characters of microorganisms. On the other hand, these interactions can also change the chemical form of nanoparticles.

1.4 Characteristics of ENMs

1.4.1 Carbonaceous Nanoparticles

Carbonaceous nanoparticles including CNTs, graphene and graphene oxide have been extensively used in industry fields such as pharmaceuticals, antibiotics (Gomez-Rivera, Field et al. 2012), biomedical (Seabra, Paula et al. 2014), aerospace manufacture (Baur and Silverman 2007). The carbonaceous nanoparticles can be with or without surface functionalization (Petersen, Zhang et al. 2011). Among these carbonaceous nanoparticles, CNTs are the most widely applied and dominant kinds. There are two main forms of CNTs which include the single-walled carbon nanotubes (SWCNTs) and the multi-walled carbon nanotubes (MWCNTs). While the SWCNTs usually have a diameter of a few nanometer and length of several micrometers, the MWCNTs usually have varying diameter and length. Moreover, CNTs are robust, stiff and also flexible so they are considered to be the strongest synthetic fibers (Arepalli, Nikolaev et al. 2001). CNTs surface can also be functionalized by functional groups to increase its water solubility in order to improve sorption properties (Huang, Fairbrother et al. 2014). It is because hydrophilic CNTs have better surface contact with adsorbates than hydrophobic CNTs (Huang, Tzeng et al. 2004). The attachment of metal nanoparticles can also modify CNTs surface, and increase the range of contamination treatment by remediation (Xiao, Shen et al. 2009). CNTs can also absorb natural organic matter (NOM) (Hyung and Kim 2008), inorganic metal cations and anionic pathogens (Brady-Estévez, Kang et al. 2008),

hydrophobic organic chemicals (Cho, Huang et al. 2011), and cyanotoxins (Upadhyayula, Deng et al. 2009).

1.4.2 TWEEN™ 20-Coated Ag ENM

Silver is well known as wide spectrum antimicrobial agent that has been extensively used in cosmetics, pharmaceuticals, fabrics, and other consumer products (Kim, Kuk et al. 2007, Kaegi, Voegelin et al. 2011). However, the inherent toxicity of Ag ENM has created challenges to the environment. Metal ENMS including silver tend to be easily modified by a variety of capping agents, which will change their character significantly. Ag ENM with coating agents may have greater toxicity to microorganisms and mammalian than unmodified Ag ENM (Ahamed, Karns et al. 2008, Kvitek, Vanickova et al. 2009, Panáček, Kolář et al. 2009). Tween™ 20 is a non-ionic surfactant with hydrophobic alkyl side chains. Its low toxicity makes it possible to be widely used as a detergent and emulsifier in domestic, scientific and pharmacological applications (Batteiger, Newhall et al. 1982, Alkasrawi, Eriksson et al. 2003). Thus Tween™ 20-coated nanoparticles including Ag NP can end up in the WWTP from these applications.

1.5 Models to Predict Contaminant Fate During the CAS Process

There is consensus that the applications of ENMs will keep increasing in the future, and ENMs will end up in the environment from these applications (Alvarez, Colvin et al. 2009, Wiesner, Lowry et al. 2009, Nowack, Ranville et al. 2012). In order to estimate potential risks and impacts of ENMs to the environment, it is crucial to establish models to quantitatively evaluate ENMs in complex natural media. There are efforts already been made to analytically study ENMs releasing into the environment. Critical

reviews have been published to evaluate the accessibility of quantifying ENMs in natural media or artificial complex (Klaine, Alvarez et al. 2008, Benn, Cavanagh et al. 2010, Gottschalk and Nowack 2011, Peralta-Videa, Zhao et al. 2011, Handy, Cornelis et al. 2012, Klaine, Koelmans et al. 2012, Nowack, Ranville et al. 2012). However, because of a lack of appropriate methods for detecting, characterizing and quantifying ENMs, it is very challenging for researchers to build models to predict ENMs concentration precisely (Mitrano, Lesher et al. 2012, von der Kammer, Ferguson et al. 2012). The lack of knowledge to decide the dominant parameters from physicochemical properties such as size distribution, surface character, purity and agglomeration state prevents researchers to build models for prevalent application (Gottschalk, Sun et al. 2013).

1.6 Thesis Objectives & Organization

The objective of this thesis is to build a non-linear solids-to-liquid ratio distribution model to quantitatively evaluate the concentration of ENMs in the effluent of a CAS system based upon changes in influent COD, solid retention time (SRT), and initial ENMs concentration after primary sedimentation. This model is based on a database of literature-reported experimental data for the removal of ENMs from wastewater. Additional experiments with ENMs and biomass were conducted to fill in data gaps in the literature for MWCNTs, graphene, graphene oxide, and a specific type of silver nanoparticle (Tween™ 20 coated AgNP) used by a group of researchers on our LCnano research project. This model also contains kinetics study of the CAS reactor's performance when the operational condition changes.

The thesis contains five chapters. Chapter 2 contains standard operation protocols for nanoparticles and biomass distribution experiment. Chapters 3 presents experiment of

interaction of carbonaceous nanoparticles, Tween-20 silver nanoparticles with biomass, and it also contains the detection methods of ENMs. Chapter 4 contains the CAS model and the effluent ENMs concentration from the CAS reactor based on different operation conditions. Chapter 5 contains summary and conclusions of the thesis.

CHAPTER 2

STANDARD OPERATION PROTOCOL (SOP) FOR NANOPARTICLE – BIOMASS INTERACTION

The purpose of this experiment is to determine the removal efficiency of ENMs by biomass under conditions that simulate the CAS process. This SOP includes: 1. preparation of glassware, buffer solution and biomass. 2. Determination of total suspended solid (TSS) of biomass. 3. Nanoparticle-biomass batch interaction experiment. 4. Nanoparticle concentration determination experiment.

2.1 Glassware and Buffer Solution Preparation

1. Wash two 1 L volumetric flasks, three 1 L glass bottles, ten 100 mL Erlenmeyer flasks with nanopure water, then dry them in the oven at 60℃.
2. Make 1 L of 1 mM $NaHCO_3$ and 1 L of 10 mM NaCl + 4 mM $NaHCO_3$ solution, store the two kinds of solution in two 1 L glass bottles separately.

2.2 Biomass Stock Preparation

1. Collect fresh biomass from the SBR tank in the laboratory or raw activated sludge from full scale WWTP into 1 L Nalgene bottle. Dispense 30 mL biomass to a set of 50 mL plastic centrifuge vials.
2. Add 10 mL of the 10 mM NaCl + 4 mM $NaHCO_3$ solution as wash buffer into each vial, shake the vials to resuspend solids.
3. Centrifuge the vials at 350 G for 15 minutes.
4. Discard the supernatant carefully, don’t discard any biomass.
5. Repeat step 2 to 4 for two more times.
6. Add 1 mM $NaHCO_3$ solution buffer into vials to the volume of 30 mL.

2.3 Determine TSS of Biomass

1. Collect fresh biomass from the SBR tank in the laboratory into glass bottles. Keep the biomass in the 4℃ refrigerator, use them in 24 hours.
2. Prepare 2 pieces of 0.45 μm Whatman® nylon membrane filters, dry them in oven at 105℃ for 1 hour, let the filters cool down, then weigh the filters separately as W_{11}, W_{12}.
3. Apply the first filter to the vacuum and rinse with 20 mL nanopure water.
4. Filter 20 mL biomass.
5. Carefully detach the filters from vacuum, make sure no biomass are left on vacuum or spilled.
6. Repeat step 3 to 5 for the second filter.
7. Dry the filters in oven at 105℃ for 3 hours, let the filters cool down, then weigh the filters separately as W_{21}, W_{22}.
8. Calculate TSS by Eq. (2.1).

$$\text{TSS}\left(\frac{\text{mg}}{\text{L}}\right) = \frac{\frac{(W21-W11)\,g}{20\,mL}+\frac{(W22-W12)\,g}{20\,mL}}{2} * \frac{1000\,mg}{g} * \frac{1000\,mL}{L} \qquad \text{Eq. (2.1)}$$

2.4 Determine TSS of Biomass by UV-Vis

1. After TSS is determined, use UV-Vis full wavelength scan to determine the absorbance of the biomass sample from 200 nm to 780 nm.
2. Determine absorbance peak of biomass sample by UV-Vis. For example, if the absorbance peak is 680 nm, then extract the absorbance data at 680 nm as OD_{680}.

3. Take the OD_{680} data of biomass samples with different TSS value. Plot graph with data points of OD_{680} as x-axis, TSS as y-axis. Make linear standard curve from these data points. Example is shown as Figure 2.

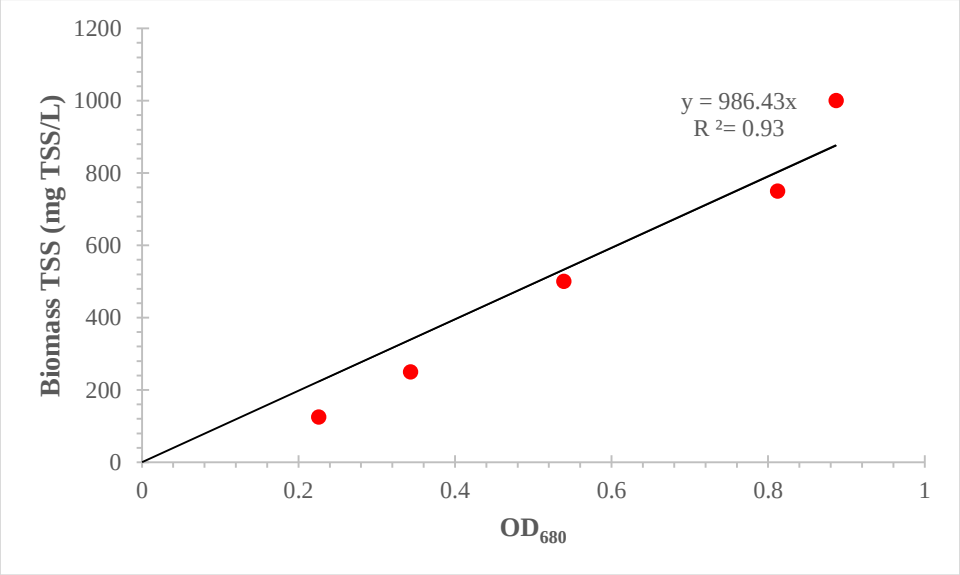

Figure 2. Standard curve of TSS determination by UV-Vis at 680 nm

4. The standard curve can be used to calculate TSS value by determine the OD_{680} value of biomass sample. This method is convenient and time-saving once the standard curve is built. .

2.5 Nanoparticle – Biomass Batch Interaction Experiment Protocol on Orbital Shaker

1. After the biomass stock has been washed and stored, label Erlenmeyer flasks with number, and prepare 1 mM $NaHCO_3$ as buffer solution, sonicate NP suspension by using the bath sonicator.

2. Add determined volume of 1 mM $NaHCO_3$ as buffer solution into all Erlenmeyer flasks.
3. Add determined volume of washed stock biomass to each sample and biomass only control group.
4. Add determined volume of sonicated NP into each sample and NP only control group.
5. Put all Erlenmeyer flasks on orbital shaker, run the shaker at 150 rpm for 3 hours in order to simulate the activated sludge process in the CAS system.
6. After the shaking process, take all Erlenmeyer flasks on the bench, let them settle for 30 minutes in order the simulate the second clarifier settling process in the CAS system.
7. Take determined volume of supernatant from each Erlenmyer flask into vials, store at 4℃ for further analyze.

2.6 NP Measurement by UV-Vis

1. Make pure NP samples with determined concentration of 0.05 mg/L, 0.1 mg/L, 0.2 mg/L 0.5 mg/L, 1 mg/L, 2 mg/L, 5 mg/L.
2. Take samples to UV-Vis full wavelength scan to determine the absorbance of the samples from 200 nm to 780 nm.
3. Determine absorbance peak of samples by UV-Vis. For example, the samples of Tween™ 20 Ag NP and biomass interaction experiment has a absorbance peak at 415 nm.

4. Take the OD_{415} data of samples with different TSS value. Plot graph with data points of OD_{415} as x-axis, absorbance as y-axis. Make linear standard curve from these data points.
5. Determine OD_{415} value for all experiment samples, use the standard curve to calculate NP concentration in all experiment samples.

CHAPTER 3

INTERACTION OF CARBONACEOUS NANOMATERIALS WITH WASTEWATER BIOMASS

This chapter is from a accepted paper on Frontiers of Environmental Science & Engineering entitled "Interaction of Carbonaceous Nanomaterials with Wastewater Biomass" by Yu Yang, Zhicheng Yu, Takayuki Nosaka, Kyle Doudrick, Kiril Hristovski, Pierre Herckes, Paul Westerhoff. My contribution was designing and conducting the experiment of interaction of carbonaceous nanomaterials with wastewater biomass. I also quantitatively determined the concentration of nanomaterials in the result samples with other authors of this paper.

3.1 Introduction

Carbon nanotubes (CNTs) and graphene are increasingly incorporated in consumer products and industrial processes, including flame retardant materials (U.S.EPA 2013), aerospace materials (Baur and Silverman 2007), and other applications (Petersen, Zhang et al. 2011). These carbonaceous nanomaterials (NMs) are mainly composed of aromatic carbon structure with or without surface functionalization (Petersen, Zhang et al. 2011). Multi-walled CNTs (MWCNTs) are the most dominant and representative class of these carbonaceous NMs (Piccinno, Gottschalk et al. 2012), and their estimated production is 55–1,101tons/year (Hendren, Mesnard et al. 2011). Although there are no substantiated reports confirming the annual production of graphene on a global scale, the graphene market is anticipated to reach $149.9 million by 2020 (Clark and Mallick 2014). This rapid growth in carbonaceous NM production and markets will inevitably increase their release into the environment.

Nanomaterial release to the environment occurs throughout all life cycle stages, starting with synthesis and purification, incorporation into products, recycling of manufacturing waste, product usage, and ending with disposal (Petersen, Zhang et al. 2011, Nowack, David et al. 2013). NMs released to wastewater eventually enter wastewater treatment plants (WWTPs). As such, the NM manufactures in the United States must consider discharges of NMs to sewers and removal at WWTPs. However, limited information exists about the removal of MWCNTs and graphene in WWTPs (Petersen, Zhang et al. 2011). Modeling results estimate that MWCNTs are released to receiving waters at low concentrations (i.e., less than 1 mg/L) (Mueller and Nowack 2008, Gottschalk, Sonderer et al. 2009); however the ability of WWTPs to remove carbonaceous NMs needs to be verified. In the absence of data, manufacturers must assume zero NM removal from water across WWTPs in the United States (U.S.EPA 2010). Exploring the removal of carbonaceous NMs by municipal WWTPs is necessary to close the knowledge gap.

The main challenge of determining NM removal stems from barriers to quantifying NMs in wastewater or biomass matrices. Until recently, measuring carbonaceous NMs other than fullerene (C_{60}) derivatives by mass spectroscopy methods has not been reported (Herrero-Latorre, Alvarez-Mendez et al. 2014). Single-walled CNTs were recently measured using single particle ICP-MS, where catalysts in the single-walled CNTs (e.g., yttrium) were surrogates for the CNTs, but this is not feasible with most multi-wall CNTs because they use more earth abundant metals in biomass which can cause background interference. MWCNTs with unique isotopic carbon ratios have been quantified using combustion followed by mass spectroscopy (Plata, Reddy et al. 2012),

which cannot be applied in our study due to the complicated background carbon in the biomass. We and others have developed a programmable thermal analysis (PTA) method for MWCNTs(Doudrick, Herckes et al. 2012) and have applied this method to quantify MWCNTs in rat lung tissue (Doudrick, Corson et al. 2013) and graphene oxide (GO) in biomass (Doudrick, Nosaka et al. 2015). When using PTA to quantify carbonaceous NMs in complex organic matrices, removal or digestion of background carbon is required to reduce carbon interference or false positives. We have demonstrated PTA to analyze graphene in matrix with low biomass concentration (e.g., 50 mg/L, total suspended solids, TSS). However, challenges still existed when analyzing MWCNTs and GO in the presence of high biomass concentration (e.g., ≥1,000 mg TSS/L). Alternatively, as will be discussed below, MWCNTs and GO are easily dispersed in solution and yield UV-Vis absorption spectra (Doudrick, Nosaka et al. 2015) that did not interfere with soluble organics, allowing UV-Vis to be used for quantification of the supernatant mass of MWCNTs and GO.

The aim of this study was to determine the removal of carbonaceous NMs by the wastewater biomass, including MWCNTs, GO, and graphene. Batch biosorption studies were conducted in a range of biomass concentration (e.g., 50 – 3,000 mg TSS/L). The mass of carbonaceous NMs adsorbed to biomass or retained in the liquid was quantified by UV-Vis or PTA method. Results obtained from this study provide critical information in environmental assessment and environmental exposure modeling (Mueller and Nowack 2008, Gottschalk, Sonderer et al. 2009).

3.2 Experimental Approach

3.2.1 Preparation and Characterization of Carbonaceous Nanomaterials Dispersions

GO suspension was obtained from TW Nano Materials (CA, USA) with the following characteristics provided by the manufacturer: 0.2 wt. %, >90% single layer, 0.5 - 20 μm in x-y, 1.1 nm of thickness when dispersed in water, 1:1.3 C:O ratio, >1,200 m^2/g). Because single-layer, non-oxidized graphene is hard to achieve in aqueous solution, few-layer graphene(FLG) nanoplatelet powder (N006-P, Angstron Materials, OH, USA) was chosen to represent graphene and was used as received (characteristics by manufacture: >97% carbon, <1.5% oxygen, <1.5% ash, 10-20 nm thick, <14 μm in x-y 122 direction, 21 m^2/g) (Doudrick, Nosaka et al. 2015). MWCNTs (length 5-20 μm, outer diameter 15 ± 5 nm) were obtained from Nanolab Technologies (Milpitas, CA, USA) and oxidized by researchers in the lab of Dr. Howard Fairbrother at Johns Hopkins University (Smith, Wepasnick et al. 2009). Briefly, MWCNTs were oxidized in a concentrated acid mixture of sulfuric acid (98% $H_2SO_4$by mass) and nitric acid (69% HNO_3 by mass) at 70 ℃ for 8 h and in a volume ratio of sulfuric acid to nitric acid of 3:1(Yi and Chen 2011). After further washing (with deionized water) and drying, four types of MWCNTs were characterized by x-ray photoelectron spectroscopy (XPS) and showed surface oxygen contents of 3.5%, 6.4%, 7.3%, 8.3% (Cho, Smith et al. 2008). As the surface oxygen content in pristine MWCNTs was 0.4%, which was below 2% and considered as common pristine MWCNTs (Smith, Wepasnick et al. 2009). The MWCNTs with higher oxygen contents (i.e., 3.5-8.3%) were considered to be oxidized MWCNTs (O-MWCNTs) (Smith, Wepasnick et al. 2009). The dispersion of both pristine and O-MWCNTs was sonicated in a water bath sonicator for one hour, and the GO suspension was sonicated

for 5 minutes before using. The final concentrations used for all experiments were 25 mg MWCNTs/L and 25 mg GO/L.

3.2.2 Carbonaceous Nanomaterials Removal Experiments

The removal of carbonaceous NMs from wastewater liquid by wastewater biomass was examined following experimental protocols by Kiser et al. (Kiser, Ryu et al. 2010). In brief, clean activated sludge was collected from a lab-scale sequencing batch reactor seeded by activated sludge from a local WWTP. The continuous two year operation of the reactor ensures that the biomass is not externally contaminated by metals or carbonaceous NMs. Collected biomass was refrigerated at 4 ℃ and stored for less than 24 h before use. Prior to experiments, activated sludge was rinsed three times with a carbonate buffer solution (10 mM NaCl and 4 mM $NaHCO_3$) and then centrifuged (F = 350 G) for 15 minutes. The supernatant was discarded, and dewatered sludge was re-suspended in a 1 mM of $NaHCO_3$ buffer solution. The pH of mixed sludge and buffer solution was adjusted to pH 7.0 $\pm$0.2 with 0.1 mM of HCl or 0.1 mM of NaOH. After pH adjustment, the TSS of the biomass stock solution was determined using standard method (APHA, AWWA et al. 2005).

Aliquots of biomass stock solution were spiked into a series of plastic vials containing NMs and buffered with 1 mM $NaHCO_3$ solution. The final biomass concentration ranged from 50 mg TSS/L to 3,000 mg TSS/L, where the maximum biomass concentration used in this study is similar to the typical activated sludge concentration in a WWTP (Grady, Daigger et al. 1999). Positive controls included NMs and buffer solution without biomass, and the negative control included only clean

biomass and buffer solution. The final volume of all aliquots was 30 mL. The initial concentrations in the mixed liquor were 25 mg GO/L and 25 mg MWCNTs/L.

After mixing NMs and biomass, the suspensions were capped in tubes and agitated on a wrist-action shaker for3 hours, which is a typical duration for the aeration stage in a WWTP. Following agitation, the mixed suspension was settled by gravity for 30 minutes (Kiser, Ryu et al. 2010). For GO and CNT experiments, a supernatant aliquot of 6 mL was pipetted out from each vessel for further analysis. The supernatant was centrifuged for 5 min at F = 1,000 G to remove any remaining suspended particles and then analyzed by UV-Vis method.

Experiments with FLG and clean biomass followed the same protocols except that different NM concentrations were used. To facilitate analysis, the initial concentrations of FLG ranged from 0.3 to 8.3 mg C/L. A single biomass concentration of 50 mg TSS/L was applied for all the FLG experiments. The negative control contained only biomass without any FLG. After 3 hours of mixing and 30minutes of gravity settling, 26 mL of supernatant was carefully removed with a pipette. The remaining suspension of 4 mL was centrifuged at F =21,293 G for 10 minutes, and the supernatant was discarded. The remaining biomass was used for PTA analysis.

3.2.3 Quantificationof the Carbonaceous Nanomaterials

MWCNTs and GO in the supernatant were quantified using a UV-Vis light scattering spectrophotometer (MultiSpec-1501, Shimadzu, Japan) with minimum detection limit of 1 mg/L. For FLG studies, biomass was digested in alkaline solution to eliminate excess biomass and facilitate separation of FLG before it was quantified using PTA (Doudrick, Nosaka et al. 2015). The detailed PTA analysis is described by Doudrick

et al.(Doudrick, Herckes et al. 2012, Doudrick, Nosaka et al. 2015). Briefly, 1 mL of SOLVABLE™ (aqueous based solubilizer, PerkinElmer, MA, USA) was added to the biomass remaining after centrifugation. The mixture was then incubated for 24 hours at 60 ℃, and then 2% (by weight) of sodium borohydride (99.99%, Sigma Aldrich, MO, USA) was added to the mixture. In order to remove any residual surfactant from SOLVABLE™, the rinsing procedure consisted of centrifugation at F = 21,293 G for 10 minutes followed by decanting and addition of 1 mL of nanopure™ water (Barnstead, 18.2MΩ·cm). The suspension was agitated for 1 minute using a vortex agitator, and then the centrifugation step was repeated. After centrifugation and removal of the supernatant, the final pellet that formed at the bottom of the centrifuge tube was suspended in 0.1 mL of nanopure water and used for PTA analysis.

3.3 Results and Discussion

3.3.1 Carbonaceous Nanomaterial Analysis in Presence of Wastewater Biomass

In the wastewater biomass experiments, it was possible to measure NMs either in solution or in the biomass to calculate the removal of NMs from the liquid phase. However, both measurements face potential interferences when analyzing elemental carbon (i.e., NMs) in the presence of large amounts of dissolved and/or particulate organic matter associated with soluble microbial products (SMPs), cellular debris, and/or intact cells. Because NMs in supernatant are representative of the discharge from a full scale WWTP into receiving water, we preferred analyzing NMs in the supernatant when possible.

To identify the specific wavelength for quantification, UV-Vis spectra between 200 and 700 nm were obtained for three suspensions of NMs and the supernatant of biomass

and are shown in Figure 3(a). In the absence of NMs, soluble organics in a supernatant sample collected from a test with 1,000 mg TSS/L had minimal UV-Vis response at wavelengths longer than 300 nm. Thus absorbance at wavelengths equal to or above 300 nm can be used to quantify the concentration of NMs without the interference from biomass. GO exhibited peaks at both 230 and 300 nm, which were also observed in other studies (Shin, Kim et al. 2009, Zhang, Yang et al. 2010). To avoid interference from biomass supernatant background, 300 nm was used for GO quantification. No obvious peak was observed for the suspension of MWCNTs, and the wavelength of 400 nm was applied for quantification as it showed a large absorbance value.

Calibration curves were obtained by us using UV-Vis for both GO and MWCNTs with a minimum detection limit of 1 mg/L. Pristine and O-MWCNTs with lower oxygen content (i.e., $\leq$ 7.3%) were not as stable as O-MWCNTs with 8.3% of oxygen; the former quickly aggregated and precipitated in nanopure water or 1 mM $NaHCO_3$ even after a 1-h water bath sonication. Five types of MWCNTs were tested in this study, while O-MWCNTs with 8.3% of oxygen were quantifiable using a UV-Vis calibration curve. In the removal experiments, negative controls without NMs were conducted over a wide range of biomass concentrations (50 to 3,000 mg TSS/L). By subtracting the absorbance of the background biomass supernatant, the concentrations of GO or O-MWCNTs in supernatant could be quantified using UV-Vis absorption at 300 nm for GO and 400 nm for O-MWCNTs.

FLG at 20 mg/L showed no specific absorption/scattering peak, and the highest absorbance between 200 and 700 nm was approximately 0.12 at 400 nm. Also, the concentration of FLG in the supernatant after biosorption was expected to very low, and

challenges existed to collect and analyze FLG in supernatant. As such, instead of using the UV-Vis method described previously, PTA was used to quantify FLG because it has a lower detection limit. As a result, we quantified FLG in settled biomass instead of the supernatant. Figure 3(b) illustrates a typical PTA thermogram on FLG in biomass. When the amount of biomass was below 50mg TSS/L, the peaks on the left attributed from biomass in Figure. 5b was negligible. Thus 50 mg TSS/L biomass led to no observable interference on the signal from FLG and was chosen for FLD distribution study in our research.

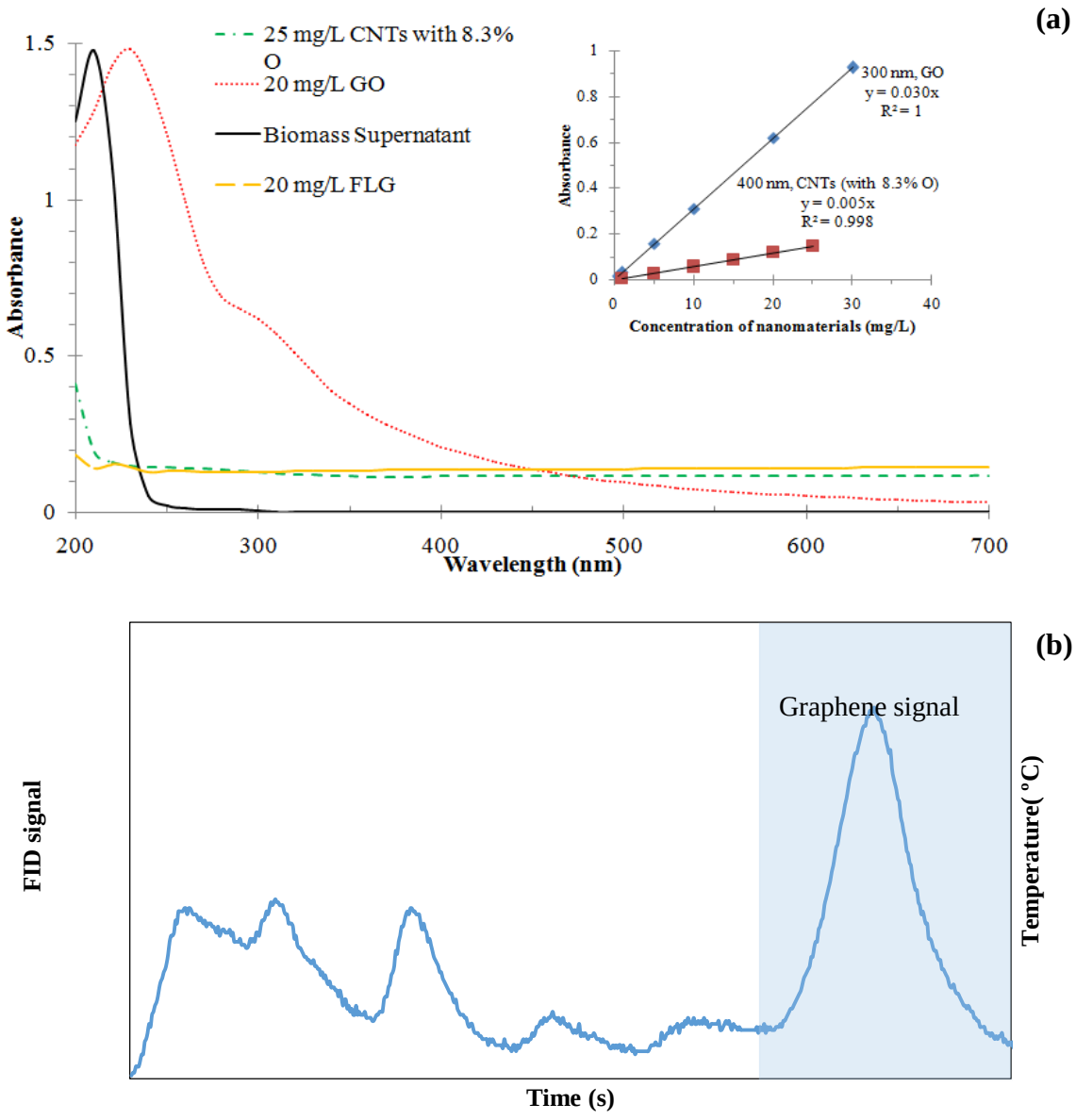

Figure 3.(a), UV-Vis characterization of graphene oxide (GO) suspension (20 mg/L), carbon nanotubes with surface oxygen content of 8.3% (25 mg/L), and biomass supernatant (after 30 minutes settling of 1,000 mg/L biomass). (b), PTA thermogram for adsorption test of FLG in biomass under He/O_2 atmosphere. Signal in shaded area (>775 ℃) is counted for FLG quantification of 50 µg.

3.3.2 Removal of Carbon Nanotubes by Wastewater Biomass

Figure 4 shows the UV-Vis spectra for the experiment with the highest oxygen containing O-MWCNTs (i.e., the most stable MWCNT) at time zero and after the test (3 hours mixing followed by 30minutes gravity settling). The O-MWCNTs were well dispersed after the water-bath sonication after a water-bath sonication. In the positive control (i.e., without biomass), the absorbance was near zero wavelengths above 250 nm, indicating complete removal of the O-MWCNTs is simply due to homo-aggregation and sedimentation. Visual observations showed a clear supernatant, thus supporting the conclusions of the UV-Vis measurements. The same process was repeated for the other three O-MWCNTs and pristine MWCNTs. We visually observed more rapid aggregation as the oxygen content of the MWCNTs decreased. Thus pristine and O- MWCNTs were nearly completely removed even without biomass. Nonetheless, the biomass experiments were performed to verify that the presence of biomass would not unexpectedly stabilize MWCNTs. For an initial O-MWCNT concentration of 25 mg/L, biomass concentrations ranging from 50 to 3,000 mg TSS/L were added. Visual observations of the biomass and O-MWCNT solutions indicated complete removal of O-MWCNTs from the supernatant. UV-Vis spectroscopy confirmed the observations, measuring < 1 mg/L MWCNTs in the supernatant at the end of the experiment. Greater than 96% removal of the O-MWCNTs with 8.3% oxygen was obtained even at the lower biomass application (50 mg/L). Because O-MWCNT suspension with 8.3% of oxygen is the most stable among five types of MWCNTs, it was concluded that >96% removal would be achieved in the simulated wastewater treatment teats for all the MWCNTs, including the pristine one, and that the presence of biomass did not hinder MWCNT removal.

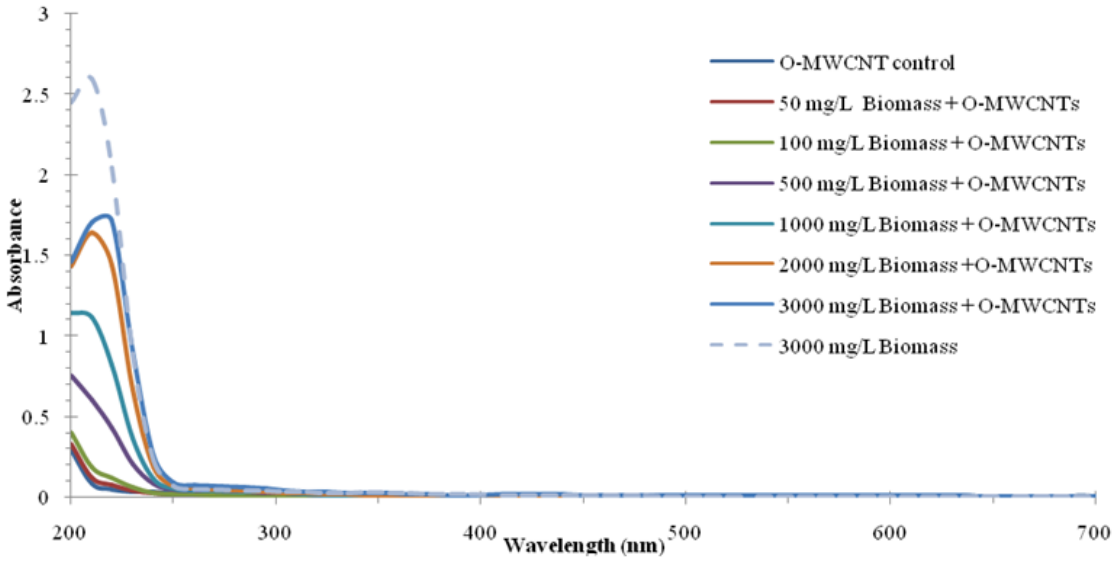

Figure 4. UV-Vis scan of supernatant after biomass absorption on O-MWCNTs with 8.3% O. Initial O-MWCNT concentration is 25 mg/L. O-MWCNT control did not include biomass but only 25 mg O-MWCNT/L.

Previous research reports a critical aggregation concentration values for MWCNTs as 25 mM NaCl, 2.6 mM $CaCl_2$, and1.5 mM $MgCl_2$ at pH 6.0 $\pm$0.2, in a time period ranging from 20 minutes to 3 hours (Saleh, Pfefferle et al. 2008), whereas we observed this to occur at less than 1 mM $NaHCO_3$ matrix (pH = 7.0, ionic strength = 1 mM) in shorter than 5 min. Nearly all wastewaters have ionic strengths above 1 mM, thus higher ionic strength in wastewater can lead to more rapid homo- or hetero-aggregation of MWCNTs with other colloids because of the dependence of electrostatic repulsion on the Debye layer thickness (Suzuki, Tanaka et al. 2002). In the prior study (Saleh, Pfefferle et al. 2008), the MWCNT suspension used in previous research was sonicated for 30 minutes, settled solids were removed, and the supernatant was used and re-sonicated – a process repeated five times (Saleh, Pfefferle et al. 2008). This process may have

significantly altered the size or surface functionality of the MWCNTs compared to this study where the pristine and O-MWCNTs were sonicated in a water bath only to form a homogeneous dispersion. Thus, different formulations of MWCNTs may experience different rates of homo-aggregation or hetero-aggregation with biomass. Because homo-aggregation rates depend upon the initial NM concentration, it is possible the rate of aggregation at lower MWCNT concentration could be much lower than the rate observed in our experiments with 25 mg/L. To work with lower MWCNT concentrations in the presence of biomass would necessitate improved analytical detection of MWCNTs dispersed in solution.

The 1-hour sonication can decrease the length of O- MWCNTs. Our unpublished data and other literatures also suggested the sonication could decrease the size of CNTs and unalter the surface oxidation state in the absence of strong oxidant [16, 17, 26]. However, even with decreased lengths of pristine MWCNTs and O-MWCNTs, 96% of them were removed from liquid phase after 3-h mixing and 0.5-h settling. Since sonication increased the stability of all MWCNT suspensions (upon observation), it is reasonably to conclude that more than 96% of pristine and O- MWCNTs could be removed from liquid phase with or without sonication.

3.3.3 Removal of Graphene Oxide by Wastewater Biomass

Unlike pristine or O-MWCNTs, GO did not undergo any measurable homo-aggregation in control experiments (i.e., no biomass). Addition of biomass led to lower GO concentrations in the supernatant (Figure 5). Less than 10% removal of GO occurs at 50 or 100 mg/L. Biomass dosages of 500 and 1,000 mg/L had 38% and 65% removal, respectively. For biomass dosages above 2,000 mg TSS/L, greater than 75% of GO was

removed from the supernatant (compared against controls of GO without biomass). When the biomass concentration was below 100 mg TSS/L, we could still find the characteristic absorption peak of GO at 230 nm [28]. As biomass concentration increased, more GO was removed. At higher concentrations of biomass, the absorption peak of GO at 230 nm disappeared and the high concentration of biomass led to another peak at 215 nm (comparable to 3,000 mg/L biomass control).

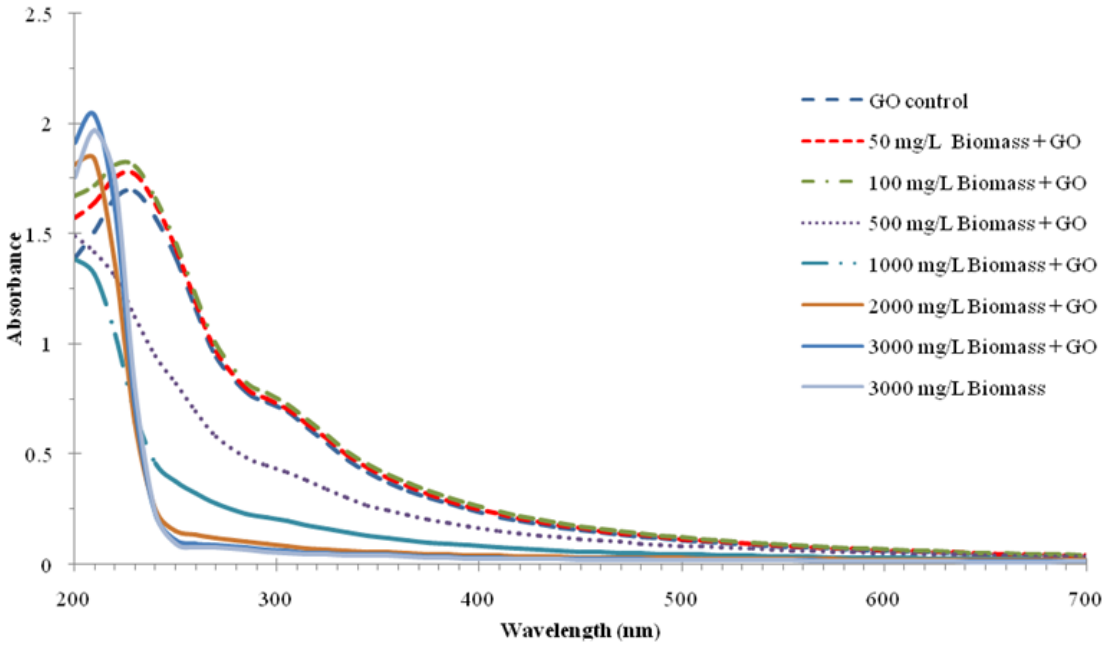

Figure 5. UV-Vis scan of supernatant after biomass absorption on graphene oxide (GO). Initial GO concentration is 25 mg/L. GO control did not include biomass but only 25 mg GO/L.

Data for GO removal as a function of biomass dosage were fit using a Freundlich model (Figure 6). By applying the Freundlich model, we did not assume equilibrium or any other thermodynamic state, but we simply applied the model as a mathematical fit of the data. Similar work has been applied elsewhere for NMs (Wiesner and Bottero 2011), oxo-anions, and other pollutants (Westerhoff and Nowack 2013). The Freundlich model

($q = 5.0\ C_s^{0.5}$) fit the observed data (R^2=0.6), where C_s is the supernatant concentration of GO and q represents a sorption density (mg GO/g TSS).

To explore the dominant interaction between GO and biomass, the total surface area of GO and bacteria in biomass was calculated. Our previous results using QPCR (Yang, Chen et al. 2012) show the total bacteria is approximately 1.0×10^9 cells/mL and the total archaea is approximately 1.0×10^7 cells/mL in the biomass of 3,000 mg TSS/L. Assuming the each cell has a similar size to a *E.coli* cell, we can estimate the total surface area of microorganism for biomass by multiplying the number of cells with the surface area of a *E.coli* cell. As a rod-shaped *E.coli* cell has surface area of approximately 0.39 μm^2(0.5 μm in width by 2 μm in length) (Neidhardt 1996), the total surface area of microbes is approximately 3.94 cm^2/mL for 3,000 mg TSS/L. Additionally, the low ionic strength of matrix (1mM $NaHCO_3$) would unlikely lead to fold or aggregation of GO, since other literature reported 50 mM of copper ion (i.e., Cu^{2+}) and above would be able to cause folding and aggregation of GO(Yang, Chang et al. 2010). Thus the total surface area of GO (surface area from information provided by manufacture, 1200 m^2/g) can be proportionally calculated to be about 300 cm^2/mL, which was much higher than that of biomass at 3,000 mg TSS/L. Therefore, the interaction among GO NMs likely dominated in the distribution process, though the carboxyl and hydroxyl group on the surface of GO(He, Klinowski et al. 1998) might hinder the aggregation of GO.

3.3.4 Few Layer Graphene Removal by Biomass

The suspension of FLG was relatively stable after 30-min water bath sonication, and there was virtually no settling of FLG after one hour. At the end of the experiments, FLG was measured in the settled biomass and compared with the MWCNT or GO that was

quantified in the supernatant. Experiments with FLG were conducted with a constant biomass concentration of 50 mg TSS/L (see above) and variable FLG concentrations. In these experiments, the percentage FLG removed was nearly constant across the range of FLG concentrations tested. FLG removal averaged 11 ± 3% (range: 8 to 16%). Consequently, when the data were plotted and fit by a Freundlich model ($q = 2.2\ C_s^{1.1}$; $R^2 = 0.94$, Figure 8), the model exponent is nearly unity, which indicates a linear distribution of FLG between the supernatant and biomass. This was somewhat unexpected unless the FLG completely covered the biomass surface – even at the lowest FLG concentration – in which case the near unity exponent may represent interaction of FLG with similar FLG NMs orientated on the biomass surface. Figure 8 also clearly shows that more FLG can be removed by biomass compared to GO ($q_{FLG} > q_{GO}$), when Cs concentration was about 6-7 mg/L.

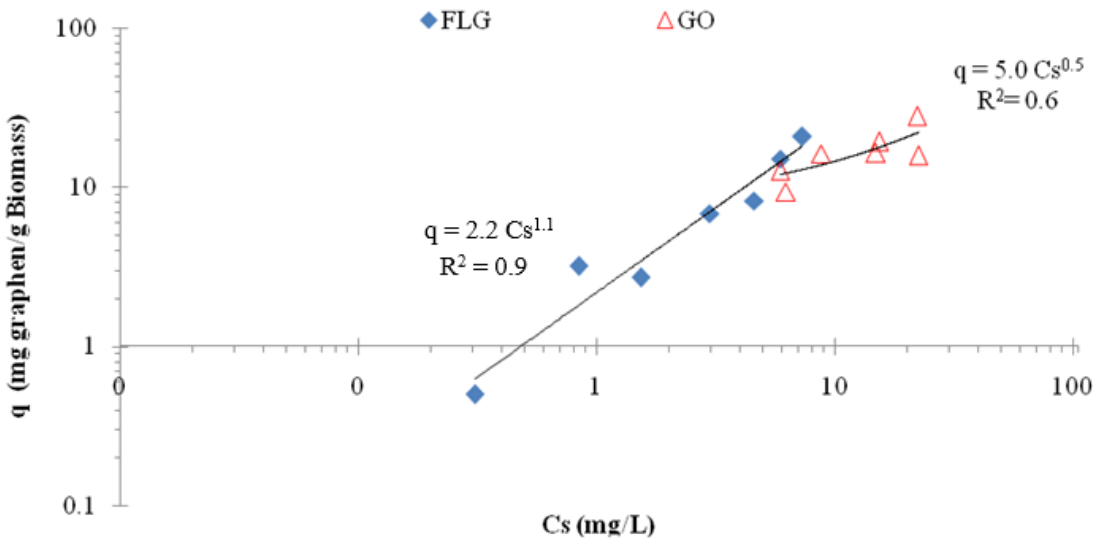

Figure 6. Analysis using a Freundlich model of the supernatant NM (i.e., GO and FLG) concentrations (Cs, mg/L) versus the amount of NM in the biomass (q, mg NM/mg TSS). The initial concentration of GO was 25 mg/L with varied biomass concentration (50 – 3,000 mg TSS/L). The initial concentration of FLG was 0.3- 8.3 mg/L with a fixed biomass concentration of 50 mg/L.

A similar calculation was conducted on the total surface area of FLG NMs and bacteria in biomass, to examine the dominant interaction in the suspension. As shown above, the total surface area of microbes in 3,000 mg TSS/L biomass is 3.94 cm^2/mL. Proportionally, 50 mg TSS/L biomass will have a surface area of approximately 6.56 × 10^{-2} cm^2/mL. The total surface area in 0.3 mg/L FLG (surface area, 21 m^2/g) is approximately 63 cm^2/mL, which is at least 100 fold larger than the surface area of microbes in 50 mg/L biomass. Therefore, interaction of FLG with other FLG NMs likely occurred, and the aggregates of FLGs covered the surface of microbes in the biomass. These experiments raise a number of interesting mechanistic questions that will be investigated in the future. With the current dataset, we can conclude quantitatively that >84% of the FLG was removed by 50 mg TSS/L of biomass. It is reasonable to expect

FLG removal would increase at higher biomass concentrations, but current analytical methods limit these quantitative assessments.

3.3.5 Removal of Carbonaceous Nanomaterials by Biomass

Table 2 summarizes the percentage removal by wastewater biomass of common carbonaceous NMs, including MWCNTs, FLGs, GO, fullerene, and functionalized fullerene. Except GO and functionalized fullerene, all other carbonaceous NMs could have more than 96% removal in the presence of 1,000 mg/L biomass. GO removal was 65% with an initial concentration of 25 mg GO/L and a biomass concentration of 1,000 mg/L. Functionalized fullerene (initial concentration as 3 mg C/L) has a 14% of removal in the presence of 400 mg/L biomass. Previous results indicate the surface functionalization/oxidation could affect the stability and removal rates of carbon nanomaterials in biomass absorption process (Kiser, Ryu et al. 2010, Petersen, Zhang et al. 2011).

Table 2. Percentage Removal of Nanomaterials by the Wastewater Biomass

Nanomaterials	Diameter of NMs (nm)	Initial concentration of NMs(mg/L)	Biomass concentration (mg/L)	Percentage removal	References
Multi-walled CNTs with 0.4% - 8.3% oxygen	12	25	1,000	>96 %	this study
Graphene oxide (GO)	1.1[a]	25	1,000	65%	this study
Few Layer Graphene (FLG)	10 – 20[a]	1	50	16%	this study
Fullerene (aq-nC_{60})	88	4	400	90%	(Kiser, Ryu et al. 2010)

Nanomaterials	Diameter of NMs (nm)	Initial concentration of NMs(mg/L)	Biomass concentration (mg/L)	Percentage removal	References
Functionalized fullerene ($nC_{60}(OH)_x$)	48	12	400	14%	(Kiser, Ryu et al. 2010)
Fullerene	88	0.07-2	500-2,000	95%	(Wang, Westerhoff et al. 2012)
CNTs				90-97% [b]	(Mueller and Nowack 2008)
General nanomaterials				32-77% [b]	(Keller and Lazareva 2014)

[a] represents thickness of NMs.
[b] represents assumed value used in modeling.

The specific mechanism governing biosorption of carbonaceous NMs on biomass is not clear yet, though the interaction between NMs and extracellular polymeric substances (EPS, one of most important sources of organic matters) is considered a driving force (Chen and Elimelech 2009, Kiser, Ryu et al. 2010). The EPS in the biomass contains a large portion of hydrophobic materials, which can enhance the stability of fullerene in the suspension (Kiser, Ryu et al. 2010). EPS can increase the electrical or steric repulsion (Becker and Foundation 2004) when interacting with carbonaceous NMs containing organic functional group on the surface. Thus GO with carboxyl group(He, Klinowski et al. 1998) showed a lower removal rate from the bulk water phase. Further research is needed to elucidate how the absorption forces change with different functionalization on the surface of carbonaceous NMs.

3.4 Conclusions

This study of pristine and O- MWCNTs, GO, and FLG in presence of biomass showed different removal from the water phase. Biomass at 1,000 mg/L removed at least 65% of GO and 96% of pristine and O-MWCNTs with an initial concentrations of 25 mg C/L, while biomass at 50 mg/L remove 16% of FLG with an initial concentration of 1 mg C/L. Because activated sludge in WWTP ranges from 1,000 mg/L to 5,000 mg/L (George, L.Burton et al. 2004), it can be concluded that majority of carbonaceous NMs entering into WWTPs would associate with biomass and be removed from the water phase. Analytical challenges still exist for quantifying pristine and O-MWCNTs and GO in the presence of high concentration of biomass. Further study is needed to address the analytical challenges of quantifying GO and MWCNTs in environmental matrices.

CHAPTER 4

INTERACTION OF TWEEN 20-COATED SILVER ENGINEERED NANOMATERIAL WITH WASTEWATER BIOMASS

4.1 Introduction

Silver has been well known for its antibacterial activity for centuries. Silver nanomaterials have wide application in cosmetics, pharmaceuticals, fabrics and other consumer products as wide a spectrum antimicrobial agents (Kim, Kuk et al. 2007, Kaegi, Voegelin et al. 2011). The antibacterial character of Ag ENM increases when the size of Ag ENM decreases, and the particle shape also affects the antibacterial character (Panáček, Kvítek et al. 2006, Martínez-Castañón, Niño-Martínez et al. 2008). The majority of Ag ENM in consumer products will be released into sewer systems and end up in WWTP (Blaser, Scheringer et al. 2008, Mueller and Nowack 2008).

Studies have shown more than 95% of the Ag entering WWTP end up into the wastewater biomass (Shafer, Overdier et al. 1998). Ag ENM in the WWTP effluent are discharged into rivers, lakes and oceans, thus poses a potential threat to aquatic organisms. Ag ENM in the wastewater biomass often end up in land application, which exposes potential threat to terrestrial organisms (Nowack and Bucheli 2007, Brar, Verma et al. 2010).

Tween™ 20 is a non-ionic surfactant with hydrophobic alkyl side chains. Its low toxicity makes it possible to be widely used as a detergent and emulsifier in domestic, scientific and pharmacological applications (Batteiger, Newhall et al. 1982, Alkasrawi, Eriksson et al. 2003). Tween™ 20-coated nanoparticles, including Ag NP can end up in

the WWTP from these applications. The objective of this chapter is to quantify the removal efficiency of Tween™ 20-coated Ag ENM by wastewater biomass.

4.2 Experiment Method

4.2.1 Biomass Collection and Preparation

Clean biomass were collected from a lab-scale sequencing batch reaction (SBR) tank that had been continually operated and maintained for over three years. The biomass were seeded from a local full scale conventional activated sludge WWTP. Previous study has shown the biomass has the equivalent removal of ENMs as full-scale WWTP (Kiser, Ryu et al. 2010). All biomass were freshly prepared and no frozen biomass were used in the experiments. In order to minimize the effect of other extraneous material in the sludge on ENPs, the sludge was prepared by the following protocol.

Activated sludge was collected from the SBR tank and then was rinsed with buffer solution (10mM NaCl, 4mM $NaCO_3$) immediately, then it was centrifuged (F=350G) for 15 min, after that the supernatant was discarded. Then the process was repeated two more times to make sure extraneous material were washed out. Another buffer (1mM $NaCO_3$) was added into the dewatered sludge to guarantee steady pH in the biomass solution. Finally, the pH was adjusted to 7.5 ± 0.2 with 1mM HCl or NaOH.

The determination of total suspended solids was executed by following a newly developed protocol, which was customized from standard protocols (APHA, AWWA, and WEF, Standard Methods for the Examination of Water and Wastewater. 21st Edition Ed. 2005.). The specific procedure of this protocol is shown in chapter 2. A more convenient method by using UV-Vis was then developed based on the result of this protocol. A group of sludge was prepared with specific concentration, and then were

analyzed by UV-Vis with full wavelength scan. The absorption peak was found and then a standard curve was made by determining the linear relationship between sludge concentration and absorption on specific wavelength.

4.2.2 Source and Characteristic of Tween™ 20-Coated Ag ENM

The TWEEN™ 20-Coated Ag ENM was synthesized by Dune Sciences, Inc. and was prepared by researchers from the University of Oregon. The average particle size was 20±7 nm tested by TEM. The ENM was sonicated for 5 minutes in a water bath sonicator before the experiment.

4.2.3 Removal Experiment of Tween™ 20-Coated Ag ENM by Wastewater Biomass

Tween™ 20-Coated Ag ENM were spiked into a series of Erlenmeyer flasks with different concentrations of biomass within the range from 50 mg/L to 3,000 mg/L, and buffer solution (1mM $NaHCO_3$). The system volume of all Erlenmeyer flasks was controlled at 30 mL. The concentration of biomass covered the typical activated sludge concentration in WWTP. Initial concentration of Tween™ 20-Coated Ag ENM was from 970 μg/L to 2,600 μg/L.

After the sample solution were prepared, samples were processed through an agitation process in order to simulate the CAS process in WWTP. The samples of Tween™ 20-Coated Ag ENM were agitated by an orbital shaker with 150 rpm. The agitation period was set to 3 hours, which is the typical time for the aeration stage of the CAS process in WWTP. After agitation, the samples were gravitationally settled for 30 minutes, in order to simulate the process of the second clarifier in WWTP. Then, an aliquot (6 mL) of supernatant in each sample was carefully pipette out into plastic vials for further analysis.

4.2.4 Quantification Method

The supernatant of samples was then centrifuged (F=1, 000 g) for 5 min to remove any suspended particles before it was analyzed by UV-Vis. Then the samples were quantified by using UV-Vis light scattering spectrophotometer (MultiSpec-1501, Shimadzu, Japan), which has a minimum detection limit of 1 mg/L. In order to determine the optimal wavelength to quantify Tween™ 20-Coated Ag ENM concentration, pure Ag ENM samples were tested by full wavelength scan to exclude interference with biomass. The optimal wavelength for Tween™ 20-Coated Ag ENM was 415 nm (Figure 7). A standard curve was done to determine the relationship of Ag ENM concentration and absorbance at 415 NM (Figure 8). Then the concentration of in each sample was calculated by using the absorbance data and standard curve.

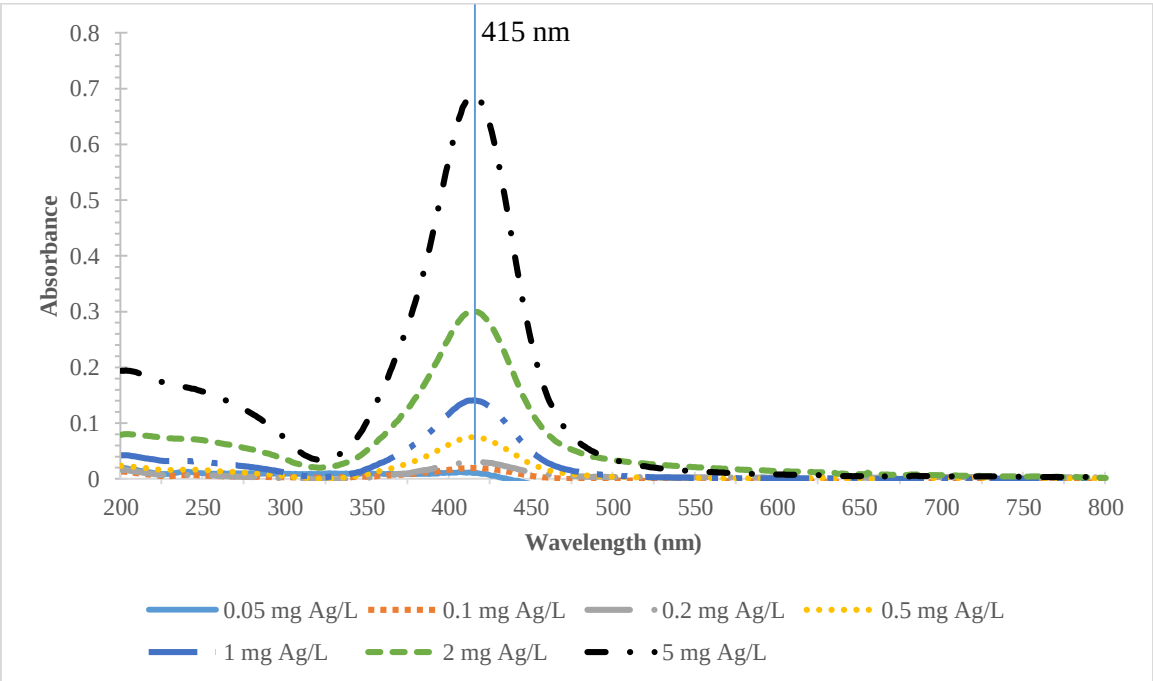

Figure 7. UV-Vis absorbance of pure Tween™ 20 Ag ENM samples with different concentrations

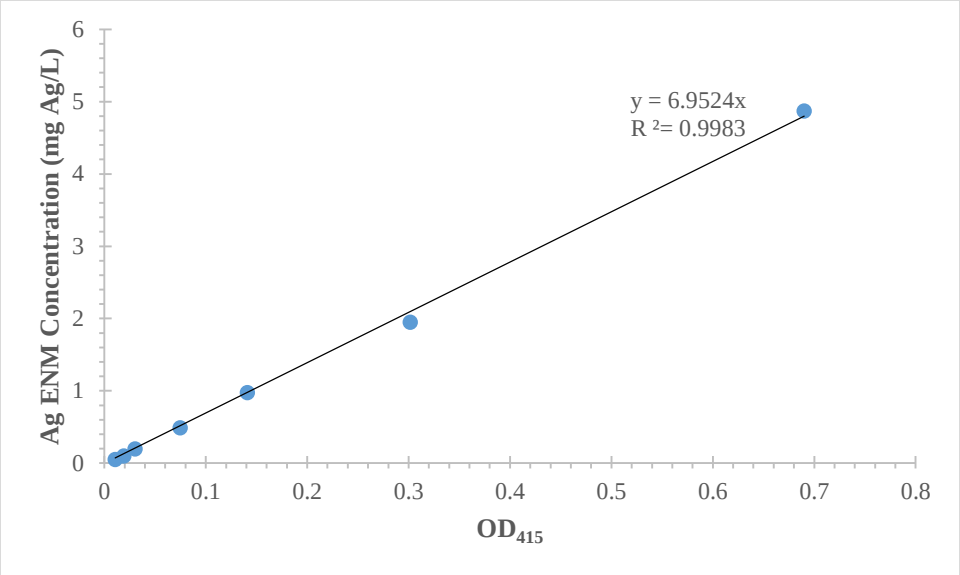

Figure 8. Standard curve of Tween™ 20 Ag ENM determination by UV-Vis at 415 nm

4.3 Results

4.3.1 Removal of Tween™ 20-Coated Ag ENM of Wastewater Biomass

Figure 9 shows the result of removal of Tween™ 20-coated Ag ENM by biomass. The absorbance of samples at 415 nm was determined by using UV-Vis, and then the Ag ENM concentration of samples were calculated by using a standard curve. There are four different initial concentrations of Tween Ag, which were 2,600 µg/L, 1,940 µg/L, 1,300 µg/L, 0.97 µg/L. The biomass concentration were from 0.5 g/L to 3 g/L. The sample of Ag control means only 970 µg/L Ag was added into the sample without biomass. Ag ENM was added in the sample without biomass. The sample of biomass control means only 1 g/L biomass was added in the sample without Ag ENM.

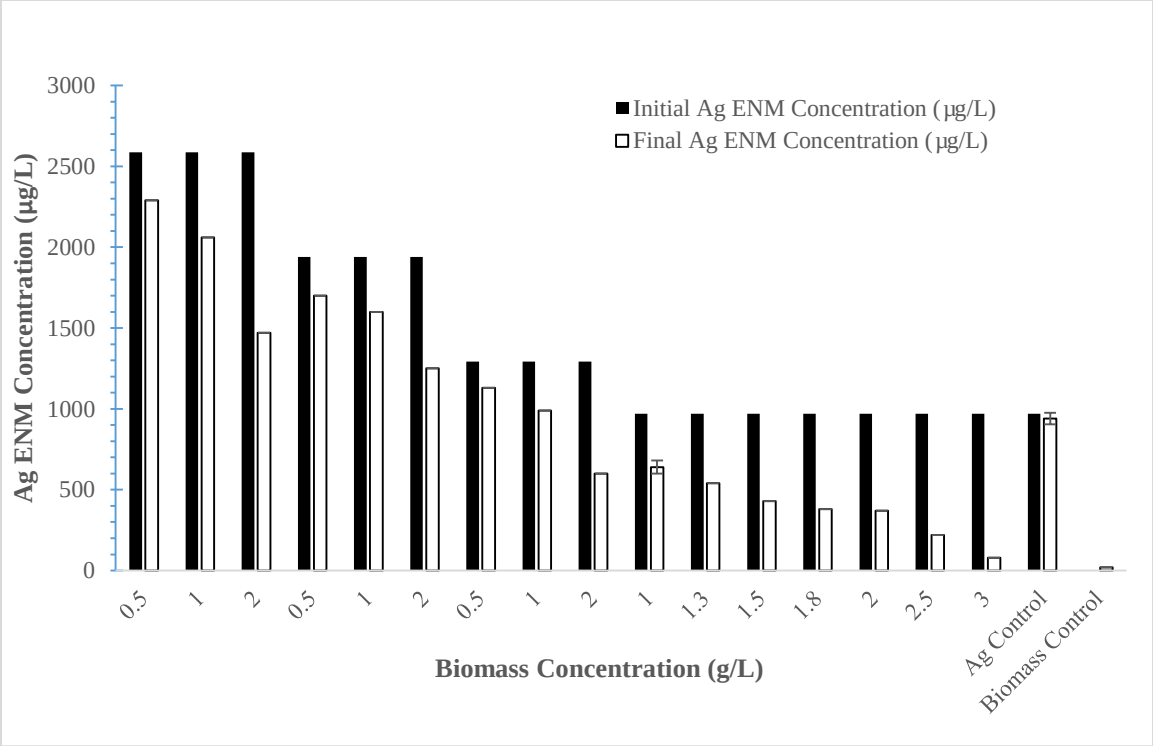

Figure 9. Result of Tween™ 20 Ag ENM Removal by Wastewater Biomass

With all samples of four different concentrations of initial Ag ENM, higher concentration of biomass had a higher removal efficiency of Ag ENM. The removal efficiency ranged from 11% to 92% in different samples. The concentration of activated sludge in WWTP ranges from 1,000 mg/L to 5,000 mg/L (George, L.Burton et al. 2004). Thus, it can be concluded that the removal of Tween™ 20 Ag ENM in WWTP will be over 50%. The removal of Ag ENM Figure 10. showed the removal of Tween™ 20 Ag ENM by fitting the data into a power function.

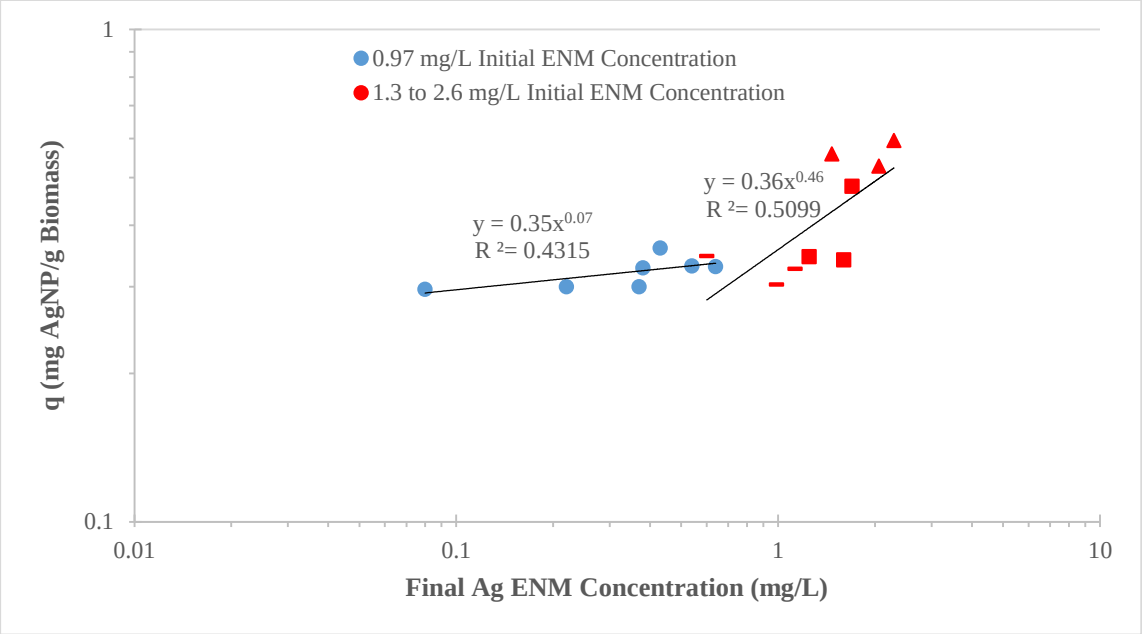

Figure 10. Power Function Relationship of Tween™ 20 Ag ENM Removal by Wastewater Biomass. Red triangles are samples with 2.6 mg/L initial Ag ENM, red squares are samples with 1.9 mg/L initial Ag ENM, red lines are samples with 1.3 mg/L initial Ag ENM.

To explore the interaction of Ag ENM and biomass, the total surface area of Ag ENM and biomass was calculated by using the same method in chapter 3. The mean size of Tween™ 20 Ag ENM was 20 nm determined by TEM. The result of spICPMS showed the total number of Ag ENM in a 10 ppt solution was 2.1×10^{-5}. Thus, the surface area of 2,600 µg/L Tween™ 20 Ag ENM was calculated as 6.86×10^{-4} cm^2/mL. This showed the surface area of Tween™ 20 Ag ENM is much less than the surface area of 50 mg/L biomass, which was 6.56×10^{-2} cm^2/mL. It showed even the highest concentration of Ag ENM in the samples has less surface area than the lowest concentration of biomass in the samples. Thus the major interaction of this experiment was between Ag ENM and

biomass for all the samples. Our results showed consistent removal efficiency with previous studies, which observed 40% to 90% removal of Ag ENM with different size and capping agent by biomass in a sequencing batch reactor (SBR) tank (Kiser, Ryu et al. 2010, Kaegi, Voegelin et al. 2011, Wang, Westerhoff et al. 2012, Yang, Wang et al. 2014).

4.4 Conclusions

The removal of Tween™ 20 Ag ENM of biomass was determined by UV-Vis with a standard curve. The result of the experiment showed the removal efficiency of Tween™ 20 Ag ENM was from 11% to 92% at an initial Ag ENM concentration from 970 μg/L to 2,600 μg/L with biomass concentration from 0.5 g/L to 3 g/L. This result shows the removal of Tween™ 20 Ag ENM is related to the biomass concentration. Biomass in regular WWTP at concentration range from 1,000 to 3,000 mg TSS/L can reach at least 50% removal of Tween™ 20 Ag ENM.

CHAPTER 5

MODEL OF ENMS REMOVAL OF THE CAS PROCESS IN WWTP

5.1 Introduction

The production, manufacture and consumer usage of ENMs have led to environmental release of ENMs. Wastewater discharges, sewage sludge, land application and waste incineration of products are the major flows that conveys ENMs to the environment (Gottschalk and Nowack 2011). Hence, monitoring ENMs removal and release at WWTP is important. However, the lack of appropriate technology to detect and quantify ENMs in the complex wastewater sludge (i.e. biomass) media or liquid effluents impedes the accessibility of ENMs concentration data from WWTP (Gottschalk, Sun et al. 2013). From a few published studies, valuable empirical data has provided accessibility to model ENMs removal at WWTP. Modeling can predict ENMs removal at different WWTP under different operational conditions, and can also predict ENMs removal efficiency during the period when operational conditions changes.

This chapter presents the development of a CAS model in Fortran code to predict solid-to-liquid ratio distribution of the concentration of ENMs in the effluent of the CAS process. I incorporated a non-linear power function relationship of Freundlich isotherm into the CAS model by adopting an iterative solving subroutine. I also collected data from published journals to create a database that shows ENMs removal by activated sludge in terms of Freundlich isotherm. The database is adapted into the model to predict ENMs effluent concentration of the CAS process under different operational conditions. I also did kinetics study of the performance of ENMs removal by the CAS model when changing operational conditions.

5.2 Model to Predict ENMs Removal Efficiency by the CAS Process

The model is built based on the analysis and design of the CAS process by Rittmann and McCarty (Rittmann, McCarty, 2001). A previous study has already built a model which focuses on membrane bioreactor (MBR) system (Kiser, Oppenheimer et al. 2010). My work builds upon the MBR model, and incorporates modifications from it to represent the character of the CAS process. I added Newton-Raphson method as numerical method to predict ENMs removal by the CAS process under different operational conditions. I also built non-linear Freundlich isotherm database of ENMs interacting with activated sludge, and fitted the database into the model.

5.2.1 Foundation of the CAS Model

The foundation of the CAS model is based on mass balance equations that were developed earlier (Laspidou and Rittmann 2002). Non-steady state mass balance equations of seven components in a single complete mixing reactor are established based on the Monod kinetics. These equations have already been modified in previous study to evaluate the performance of the MBR process study (Kiser, Oppenheimer et al. 2010). Table 3 summarizes key parameters and the units. Table 4 includes all seven non-steady state mass balance equations. Laspidou's paper has quantified the relationship of extracellular polymeric substances (EPS) and soluble microbial products (SMP) with active and inert biomass.

Table 3. Parameters definitions and units for mass balance equations (Laspidou and Rittmann 2002)

Variable	Definition	Units
b	First-order endogenous decay rate coefficient	T^{-1}
BAP	Concentration of biomass-associated products (BAP)	M_p/L^3
EPS	Concentration of EPS	M_{EPS}/L^3
f_d	Biodegradable fraction of active biomass	-
k_1	Substrate-utilization-associated products (UAP) formation rate coefficient	M_p/M_s
k_2	BAP formation rate coefficient	M_p/M_x -T
k_{EPS}	EPS formation coefficient	M_p/M_x
k_{hyd}	First-order hydrolysis rate coefficient	T^{-1}
K_{BAP}	Half-maximum-rate concentration for BAP utilization	M_p/L^3
K_s	Half-maximum-rate concentration for utilization of original substrate	M_s/L^3
K_D	Half-maximum-rate concentration for utilization of donor substrate	M_D/L^3
K_O	Half-maximum-rate concentration for O_2 consumption	M_O/L^3
K_{UAP}	Half-maximum-rate concentration for UAP utilization	M_p/L^3
Q	Flow rate	L^3/T
$\hat{q}_s$	Maximum specific substrate utilization rate for original substrate	M_s/M_x -T
$\hat{q}_D$	Maximum specific substrate utilization rate for donor substrate	M_D/M_x -T
$\hat{q}_{BAP}$	Maximum specific BAP utilization rate	M_p/M_x -T
$\hat{q}_{UAP}$	Maximum specific UAP utilization rate	M_p/M_x -T
R_{acc}	Rate of separate supply of acceptor	M_{acc}/L^3 -T
r_s	Specific substrate utilization rate	M_s/M_x -T
r_{UAP}	Specific UAP utilization rate	M_p/M_x -T
r_{BAP}	Specific BAP utilization rate	M_p/M_x -T

Variable	Definition	Units
S	Concentration of original donor substrate	M_S/L^3
UAP	Concentration of UAP	M_p/L^3
V	Volume	L^3
X_a	Concentration of active biomass	M_x/L^3
X_{res}	Concentration of true residual inert biomass	M_x/L^3
Y_s	True yield for substrate utilization	M_x/M_s
Y_p	True yield for SMP utilization	M_x/M_p

Table 4. Mass balance equations for nonsteady-state CAS model based on previous paper (Laspidou and Rittmann 2002), Q_0, Q_e, Q_w means influent flow rate, effluent flow rate, waste stream flow rate, respectively.

Equation Definition	Mass Balance Equations
Original Donor Substrate (S)	$\frac{dS}{dt} = -\hat{q}_s \left(\frac{S}{K_S + S}\right) X_a + \frac{Q_0 S_0}{V} - \frac{Q_e S}{V} - \frac{Q_w S}{V}$
Active Biomass	$\frac{dX_a}{dt} = \mathrm{Y}_S r_S (1 - k_1 - k_{EPS}) X_a + Y_p \left(\frac{\hat{q}_{UAP} UAP}{K_{UAP} + UAP} + \frac{\hat{q}_{BAP} BAP}{K_{BAP} + BAP}\right) X_a - \mathrm{b} X_a + \frac{Q_0 X_a^0}{V} - \frac{Q_e X_a}{V} - \frac{Q_w X_a}{V}$
True Residual Inert Biomass (X_{res})	$\frac{dX_{res}}{dt} = b(1 - f_d) X_a + \frac{Q_0 X_{res}^0}{V} - \frac{Q_e X_{res}}{V} - \frac{Q_w X_{res}}{V}$
Extracellular Polymeric Substances (EPS)	$\frac{dEPS}{dt} = k_{EPS} r_s X_a - k_{hyd} EPS + \frac{Q_0 EPS_0}{V} - \frac{Q_e EPS}{V} - \frac{Q_w EPS}{V}$
Utilization-associated Products (UAP)	$\frac{dUAP}{dt} = k_l r_s X_a - \frac{\hat{q}_{UAP} UAP}{K_{UAP} + UAP} X_a + \frac{Q_0 UAP_0}{V} - \frac{Q_e UAP}{V} - \frac{Q_w UAP}{V}$
Biomass-associated Products (BAP)	$\frac{dBAP}{dt} = k_{hyd} EPS - \frac{\hat{q}_{BAP} BAP}{K_{BAP} + BAP} X_a + \frac{Q_0 BAP_0}{V} - \frac{Q_e BAP}{V} - \frac{Q_w BAP}{V}$

Equation Definition	Mass Balance Equations
Acceptor Consumed (as O_2)	$\frac{dO_2}{dt} = -f_d b\left(\frac{O_2}{K_0 + O_2}\right)X_a - [1 - k_1 - k_{EPS} - Y_s(1 - k_1 - k_{EPS})]r_s X_a - (1 - Y_p)\left(\frac{\hat{q}_{UAP} UAP}{K_{UAP} + UAP}\right)\left(\frac{O_2}{K_0 + O_2}\right)X_a - (1 - Y_p)\left(\frac{\hat{q}_{BAP} BAP}{K_{BAP} + BAP}\right)\left(\frac{O_2}{K_0 + O_2}\right)X_a + \frac{QO_2^0}{V} - \frac{QO_2}{V} + R_{acc}$

In order to quantify the parameters in the model at steady state, pervious study has built another model based on the non-steady state mass balance equations in Laspidou's paper (Kiser, Oppenheimer et al. 2010). Kiser's model was made by discretizing the set of non-steady state mass balance equations and then using a small time step and constant input to solve the equations until the results reach steady-state values. The author had also developed a model to represent the performance of the CAS reactor by using the same discretization method (Kiser 2011). My model has adopted the CAS model from Kiser's paper to predict ENMs removal efficiency by the CAS reactor. Moreover, I added Newton-Raphson method as numerical method to predict ENMs removal by the CAS process based on non-linear Freundlich isotherms. I also studied the kinetics of the CAS reactor to determine the change of performance during the change of operational condition, and I studied the removal efficiency of ENMs by the CAS reactor before it reaches steady state.

5.2.2 Freundlich Isotherm

The removal of ENMs of wastewater biomass is mainly through adsorption or aggregation process. In order to quantify the adsorption efficiency of ENMs by biomass, the Freundlich isotherm is applied in the model. The Freundlich isotherm is applicable for non-ideal heterogeneous sorption (Freundlich 1906). Hence, it is able to represent the adsorption process of ENMs to complex components of wastewater. The typical form of the Freundlich isotherm can be represented as Eq. (5.1):

$$q_A = K{C_A}^{1/n} \tag{5.1}$$

Where q_A is the mass of ENMs that is adsorbed by per unit mass of biomass (mg ENM/g biomass), C_A is the concentration of ENMs in the liquid phase after the adsorption experiment (mg ENM/L). K is the adsorption capacity parameter (mg ENM/g biomass)(L/mg ENM)$^{1/n}$, and 1/n is the unitless adsorption intensity parameter. The Freundlich isotherm is often plotted on log scale in linear form for the convenience of observation. The linear form of the Freundlich isotherm can be represented as Eq. (5.2).

$$\log(q_A) = \log(K) + \frac{1}{n}\log(C_A) \tag{5.2}$$

When the adsorption intensity parameter is approximately 1, the adsorption process can be considered as linear. If the adsorption intensity parameter does not approach 1, the adsorption process must be considered as nonlinear.

4.2.3 Mass Balance of Flow in CAS Model

In the CAS model, the mass of adsorbed ENMs per unit time can be represented as Eq. (5.3).

$$M = K{C_A}^{1/n}X_v Q \tag{5.3}$$

Where X_v is the total suspended solids (TSS) concentration (mg TSS/L) of activated sludge, and Q is the CAS reactor influent flow rate (L/d). In general terms, assuming sorption is the only removal mechanism, the mass balance of flow in the CAS model can be represented as Eq. (5.4):

$$Q_0 C_0 = K {C_A}^{1/n} (X_v^e Q_e + X_v^w Q_w) + C_A Q_e + C_A Q_w \quad (5.4)$$

Where Q_0 is the influent flow rate of the CAS reactor (L/d), C_0 is the influent ENMs concentration (mg ENM/L). X_v^e is the effluent biomass concentration of the second clarifier (mg biomass/L), and Q_e is the effluent flow rate of the second clarifier (L/d). X_v^w is the biomass concentration in the waste stream (mg biomass/L), and Q_w is the flow rate of waste stream (L/d). It is essential to show the mass balance of ENM in order to justify the result effluent ENM concentration of the model. An example mass balance of ENM is included in the appendix.

To solve this equation and get the result of C_A, the mass balance equation can be rearranged as Eq. (5.5):

$$C_A = \frac{Q_0 C_0 - K {C_A}^{1/n} (X_v^e Q_e + X_v^w Q_w)}{Q_e + Q_w} \quad (5.5)$$

An iterative numerical approach is required to solve this equation. Also, this iterative numerical approach should ensure convergence on roots. Newton-Raphson method is qualified for both requirements, and the method is applied into the model.

The effluent concentration of ENM is represented as Eq. (5.6), which include the ENM in the solid phase and liquid phase of effluent.

$$ENM\ effluent\ concentration = C_A Q_e + K {C_A}^{1/n} X_v^e Q_e \quad (5.6)$$

5.2.4 Newton-Raphson Method

The Newton-Raphson method is a root-finding algorithm that uses the first two terms of the Taylor series of a function in the vicinity of a suspected root. The Newton-Raphson method is also known as Newton's iteration, and it can be applied to computer programs by iteration to find the root. The equation for iteration can be represented as Eq.(5.7):

$$x_{n+1} = x_n - \frac{f(x_n)}{f'(x_n)} \tag{5.7}$$

In this model, the function $f(C_A)$ is represented as Eq. (5.8):

$$f(C_A) = \frac{Q_0 C_0 - K {C_A}^{1/n} (X_v^e Q_e + X_v^w Q_w)}{Q_e + Q_w} - C_A \tag{5.8}$$

Where $f'(C_A)$ is represented as Eq (5.9)

$$f'(C_A) = \frac{\frac{1}{n}(-K) {C_A}^{\left(\frac{1}{n}-1\right)} (X_v^e Q_e + X_v^w Q_w)}{Q_e + Q_w} - 1 \tag{5.9}$$

The iteration process starts off with initial value of x_0, which is C_{A0} in this case. Take x_0 into Eq.(5.7) to get the answer x_1 which is closer to the root. Then x_1 is taken into the equation in order to get a closer answer to the root as x_2. The process repeats until the change of answer is less than 1%, which means the answer is in the acceptable range of error. This method usually converges and it is much faster to perform when been applied to computer program. Hence, after it is coded into the model, it becomes the suitable iterative numerical method to predict ENMs effluent concentration.

5.2.5 Freundlich Isotherm Database

A number of studies have determined the removal efficiency of different kinds of ENMs of wastewater by different quantification methods. I built a database from data of these studies to build isotherms to represent the removal efficiency of ENMs of biomass.

The database include Freundlich isotherm adsorption capacity parameter K, adsorption intensity parameter 1/n for each ENMs. For those studies that have already made isotherms in the articles, the isotherms are directly put into this database. For those studies that have not made isotherms, the data of initial influent concentration of ENMs to WWTP or the CAS process, effluent concentration of ENMs, concentration of ENMs in the sludge, total suspended solid (TSS), volatile suspended solid (VSS), removal efficiency are extracted from these papers, then isotherms are built based on these information. Information of the characters of ENMs including particle diameter, coating material, zeta potential are also included in the database, if there is any. The pH value of reaction solution is also provided in the database. The database is shown as Table 5.

Table 5. Database of Freundlich Isotherm Parameters, ENMs Characters, Experiment ENM and Biomass Concentration, Solution Characters

ENM	ENM Size (nm)	ENM Coating	Zeta potential at pH 7 (mV)	Solution pH	Experiment Biomass Concentration (g/L)	Experiment ENM concentration (mg/L)	K (mg ENM/g biomass)(L/mg ENM)$^{1/n}$	1/n	Reference
AgNP(A)	100 to 500	None	N/A	5.8 to 7.4	N/A	0.06 to 0.49	9.0[a]	0.7	(Benn and Westerhoff 2008)
CeO_2(A)	200	None	-25	N/A	3	100	7.43	0.88	(Limbach, Bereiter et al. 2008)
SiO_2(A)	56	Tween	0	7.0	0.293	2470	ID[b]	ID	(Jarvie, Al-Obaidi et al. 2009)
TiO_2(A)	50 to 700	None	N/A	7.0	N/A	0.1 to 3.0	34.32	0.48	(Kiser, Westerhoff et al. 2009)
SiO_2-FITC	85	Fluorescein isothio-cyanate	-50	7.0	0.4	1.0 to 50.0	0.11	1.10	(Kiser, Ryu et al. 2010)
AgNP(B)	13	None	-40	7.0	0.05	0.6	ID	ID	(Kiser, Ryu et al. 2010)
aq-nC_{60}	88	None	-52	7.0	0.4	4.0	ID	ID	(Kiser, Ryu et al. 2010)
f-Ag	3	Carboxyl	-6	7.0	0.4	0.5	ID	ID	(Kiser, Ryu et al. 2010)
fn-Ag	5	Carboxyl terminated polymer	6	7.5	1.8±0.2	0.5 to 1.5	2.08	0.69	(Wang, Westerhoff et al. 2012)
TiO_2(B)	20	None	30	7.5	1.3±0.2	0.5 to 2.0	56.02	1.15	(Wang, Westerhoff et al. 2012)

ENM	ENM Size (nm)	ENM Coating	Zeta potential at pH 7 (mV)	Solution pH	Experiment Biomass Concentration (g/L)	Experiment ENM concentration (mg/L)	K (mg ENM/g biomass)(L/mg ENM)$^{1/n}$	1/n	Reference
C_{60}(A)	88	None	52	7.5	2±0.2	2.5	5.23	0.69	(Wang, Westerhoff et al. 2012)
AgNP(C)	50	None	N/A	7.5	3	0.13 to 2.4	6.33	1.0	(Kaegi, Voegelin et al. 2011)
PVA-AgNP	21	Polyvinyl alcohol (PVA)	N/A	7.5	3	40.0	ID	ID	(Yang, Chen et al. 2012)
TiO_2(C)	5 to 30	None	N/A	7.0	2	0.18 to 1.23	3.96	0.58	(Westerhoff, Song et al. 2011)
CeO_2(B)	50	None	0±15	7.0	0.248±0.05	55	ID	ID	(Gomez-Rivera, Field et al. 2012)
Car-Ag	2	Carboxyl-ate	-52.1	7.0	0.8	2.1±0.05	ID	ID	(Kiser, Ladner et al. 2012)
Cit-Ag	2.4	Citrate	-41.3	7.0	0.8	0.4	ID	ID	(Kiser, Ladner et al. 2012)
PVP-Ag	10.6	Polyvinyl-pyrrolidone (PVP)	-39.8	7.0	0.8	0.1	ID	ID	(Kiser, Ladner et al. 2012)
GA-Ag	34	Gum-arabic	-42.2	7.0	0.8	0.5	ID	ID	(Kiser, Ladner et al. 2012)
TA-Au	7.1	Tannic acid capped	-32.3	7.0	0.8	2.2±0.3	ID	ID	(Kiser, Ladner et al. 2012)
PVP-Au	8.8	Polyvinyl-pyrrolidone (PVP)	-21.5	7.0	0.8	0.9	ID	ID	(Kiser, Ladner et al. 2012)

ENM	ENM Size (nm)	ENM Coating	Zeta potential at pH 7 (mV)	Solution pH	Experiment Biomass Concentration (g/L)	Experiment ENM concentration (mg/L)	K (mg ENM/g biomass)(L/mg ENM)$^{1/n}$	1/n	Reference
Car-PS	35	Carboxyl-ate	-51.5	7.0	0.8	2.0	ID	ID	(Kiser, Ladner et al. 2012)
Sulf-PS	13	Sulfate	-39.6	7.0	0.8	2.0	ID	ID	(Kiser, Ladner et al. 2012)
aq-nC_{60}	35.5	None	N/A	7.0	0.8	3.4±0.04	ID	ID	(Kiser, Ladner et al. 2012)
Al_2O_3	50	None	N/A	7.5	N/A	0.5 to 200.0	2.77	1.09	(Rottman, Shadman et al. 2012)
CeO_2(C)	50	None	N/A	7.5	N/A	0.5 to 200.0	3.57	1.04	(Rottman, Shadman et al. 2012)
SiO_2(B)	10 to 20	None	N/A	7.5	N/A	0.5 to 200.0	0.99	1.3	(Rottman, Shadman et al. 2012)
C_{60}(B)	92	None	-40	7.0	0.279±0.025	0.2	ID	ID	(Wang, Dai et al. 2013)
TiO_2-P25	22	None	N/A	7.3	2	1.0 to 10.0	9.5	1	(Gartiser, Flach et al. 2014)
FLG	1.1	None	N/A	7.5	2	1.0	2.18	1.06	(Yang, Yu et al. 2015)
GO	10 to 20	None	N/A	7.5	2	25.0	4.99	0.47	(Yang, Yu et al. 2015)
nC_{60}	88	None	-52	7.0	2	0.07 to 2.0	108.64	1.0	(Yang, Wang et al. 2014)
Tween™ -20 AgNP	20	Tween™ 20	N/A	7.5	2	0.97 to 2.6	0.39	0.18	Original

[a] The unit is (μg ENM/g biomass)(L/ μg ENM)$^{1/n}$

[b] Insufficient data to create distribution coefficient

The data on ENMs removal efficiency of biomass in the database are the removal efficiencies that were reported by the authors of these papers. Most papers evaluated the removal efficiency of ENMs by one specific biomass concentration. The relationship of ENMs removal and biomass concentration is not linear, thus it is not possible to predict ENMs removal efficiency by different biomass concentration base on experimental data from these papers. The CAS model is applied to predict the removal efficiency of ENMs by WWTP under different situation.

5.2.6 Model strategy

The model is developed to simulate ENMs removal efficiency by the CAS reactor in typical size WWTP. The parameters of the WWTP follow general design parameters of WWTP, which are listed in Table 6. The influent flow is designed based on the capacity of City of Phoenix 91st Avenue Wastewater Treatment Plant with a treatment capacity of 230 MGD, which is about 867,000,000 L/d. Solids retention time (SRT) is the key to design the CAS reactor. SRT can affect the effluent substrate concentration, the effluent contaminant concentration, the volatile suspended solids concentration and the active biological sludge production rate. Hence, I set the SRT in applicable range from 4 days to 20 days to determine its effect on ENMs removal efficiency. Another important factor is the ratio of SRT to hydraulic retention time (HRT), which is also known as the solids-concentration ratio. Higher solids-concentration ratio means the CAS reactor can achieve higher efficiency of substrate removal with smaller reactor volume. The range of solids-concentration ratio is from 10 to 50. In general, the effluent flow of waste stream is just a few percent of the influent flow. Biomass concentration in the effluent of second clarifier is assumed to be 1% of the biomass concentration in the aeration tank.

Table 6. Design Parameters of the CAS Model

Parameter	Value	Units	Description
Q_0	867,000,000	L/d	Influent flow into the CAS reactor
V	370,000,000	L	Volume of the aeration tank
θ_x	4 to 20	d	SRT
S_0	400 to 1,000	mg COD/L	Influent COD concentration

The range of ENMs concentrations should be able to represent the realistic contaminant concentration of ENMs in wastewater. According to the review of analytical studies of ENMs, the ENMs concentrations are set in the range from 10 μg/L to 1,000 μg/L (Gottschalk, Sun et al. 2013).

The CAS model predicts ENMs effluent concentrations from the CAS reactor under four scenarios. The first scenario simulates regular operation condition of the CAS reactor, with SRT value of 5 days and ENMs influent concentration of 10 μg/L. This scenario represented the removal capability of ENMs by the CAS reactor under general operational performance. The second scenario sets the SRT value to 20 days and ENMs influent concentration to 10 μg/L. It represents the removal efficiency when SRT is very high and leads to low biomass growth rate. The third scenario sets influent COD concentration to 1,000 mg COD/L, and sets ENMs influent concentration to 10 μg/L. It can determine the ENMs removal efficiency when the CAS reactor is under the influence of high COD influent. The fourth scenario simulates worst case scenario with low SRT as 4 days, and extremely high ENMs influent concentration as 1,000 μg/L. This scenario provides information about the CAS reactor's performance under extreme pressure. Table 7 shows the parameters data of these four scenarios.

Table 7. Parameters of CAS model under four different scenarios

Scenarios	Influent ENMs Concentration (μg/L)	Influent COD Concentration (mg COD/L)	SRT (d)	SRT/HRT ratio
Regular	10	400	5	12.5
High SRT	10	400	20	50
High COD	10	1,000	5	12.5
Worst Case	1,000	400	4	10

5.3 Results

5.3.1 Kinetic Study of the CAS Model

The CAS reactor is a dynamic system with microorganisms. When the operational conditions change, it will take time for the microorganisms to accommodate to the new conditions. During this period, parameters such as TSS and effluent COD will change and eventually the parameters will reach a steady state. It is time consuming for researchers to determine the trend and exact period of this accommodation process. However, it becomes very convenient to use a model to simulate this accommodation process. The model also helps researchers to determine the ENMs removal efficiency during the accommodation process. Figure 11 shows the change of TSS and effluent COD of the CAS reactor when the influent COD change from 400 mg COD/L to 1,000 mg COD/L at the beginning, and change from 1,000 mg COD/L back to 400 mg COD/L at day 30. The change of TSS mostly happens in the first 10 days after the change of influent COD, then reaches a steady state with less than 5% fluctuation after day 11. The change of effluent COD happens mostly in the first 2 days, and reaches a steady state

with less than 5% fluctuation from the third day. The trends of change of TSS and effluent COD are similar during day 30 to day 60.

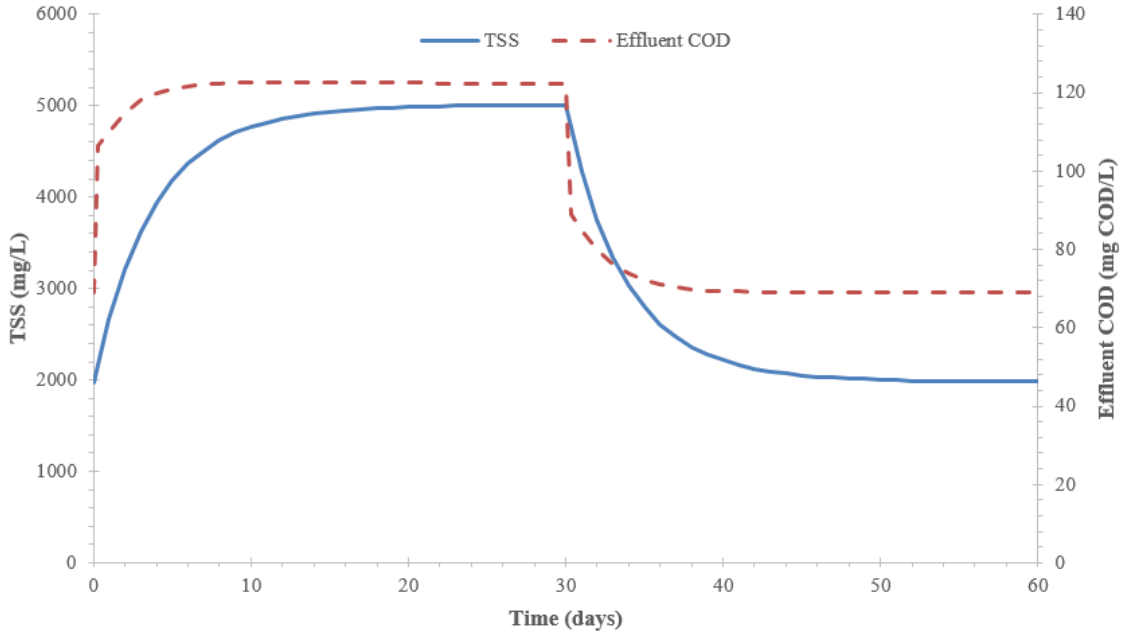

Figure 11. Change of TSS and effluent COD of the CAS reactor when influent COD change from 400 mg COD/L to 1,000 mg COD/L at the beginning, and the influent COD change from 1,000 COD/L back to 400 mg COD/L at day 30.

5.3.2 Modeled ENMs Effluent Concentration

The CAS model runs under the four scenarios. To exclude potential interference to the result, the results of ENMs effluent concentration are calculated separately. The CAS model has reached a steady state for all scenarios before the calculation of effluent ENMs concentration. In the general scenario, the value of TSS in the CAS reactor is around 2,000 mg TSS/L at steady state. In the high SRT scenario, the TSS value is 3,300 mg TSS/L. It shows that higher SRT leads to higher TSS in the CAS reactor. In the high COD scenario, the TSS value is 5,200 mg TSS/L. Thus, higher influent COD leads to higher TSS. In the worst case scenario, the TSS value is 1,700 mg TSS/L, which is the

lowest TSS value in the four scenarios. The effluent concentrations of ENMs under the four scenarios are shown as Figure 12.

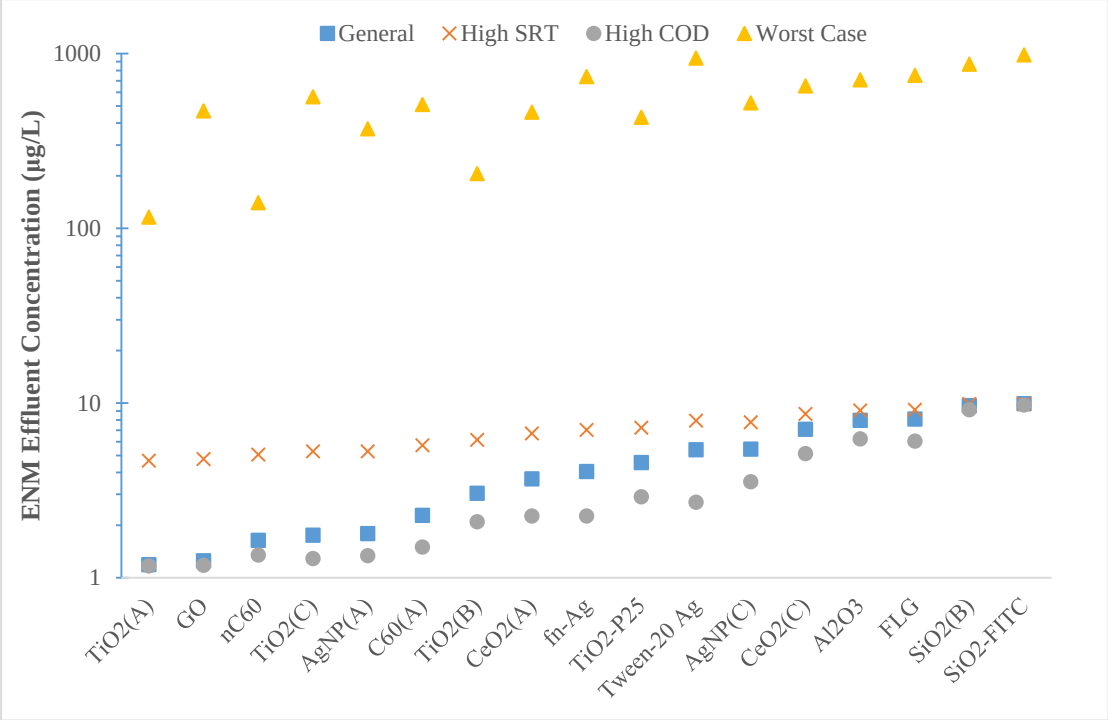

Figure 12. Modeled effluent concentration of ENMs under four scenarios

Under the four different scenarios, the effluent concentrations of ENMs are in the range of 1.19 µg/L to 984 µg/L. In the general scenario, which SRT is 5 days and influent ENMs concentration is 10 µg/L, 10 out of 17 ENMs have effluent concentration lower than 5 µg/L. Only 2 kinds of ENMs have effluent concentration higher than 9 µg/L. It indicates most kinds of ENMs can be well removed by the CAS process under general conditions.

In the high SRT scenario, which SRT equals 20 days, and ENMs influent concentration is 10 µg/L, the effluent concentrations of ENMs are higher than those in general scenario. It indicates that a higher SRT is can decrease ENMs removal efficiency.

The suggested range of SRT for general operation is 4 to 10 days, so in this scenario the SRT value is higher than general operation range. Thus, this scenario is not preferred in realistic operating condition because it will decrease the removal efficiency of ENMs. If the CAS reactor keeps a SRT value of 20 days, the percentage of nitrifying bacteria will increase and will have a very large oxygen demand that increases aeration rate and effluent COD.

In the high influent COD scenario which SRT is 5 days, and the influent COD concentration is 1,000 mg COD/L. The ENMs removal efficiency is higher than general scenario, 12 out of 17 kinds of ENMs have effluent concentration lower than 5 μg/L. Only 2 kinds of ENM have effluent concentration higher than 9 μg/L. High influent COD increases the biomass concentration in the CAS reactor, thus increases the ENMs removal. However, high influent COD also increase effluent COD concentration, which is not preferred in wastewater treatment.

In the worst case scenario which SRT is 4 days and influent concentration of ENMs is 1,000 μg/L, the effluent concentration of ENMs is in highest range of the four scenarios. The removal of ENM under worst case scenario does not always have the same trend as the removal of ENM under general scenario. For example, the removal of graphene oxide in the worst case scenario is much lower than in general scenario. It is because the importance of adsorption capacity parameter (K) will increase when the influent ENM concentration is higher. For graphene oxide, the adsorption capacity parameter is low, so the removal of graphene oxide under worst case scenario is lower. However, the worst case scenario sets the influent concentration higher than realistic situation, even if the effluent ENMs concentration is 100 μg/L, it still has 90% removal.

Moreover, the situation is unlikely to happen when influent ENMs concentration is around 1,000 μg/L. Currently most of the ENMs concentration in surface water is in the range of $1x10^{-4}$ μg/L to 100 μg/L (Gottschalk, Sun et al. 2013). If the application of ENMs keeps increasing in the future, it is possible that the concentration of ENMs in the surface water will increase to 1,000 μg/L. Until then, traditional treatment includes the CAS reactor in WWTP can still serve as capable barriers to prevent ENMs pollution to the environment.

5.3.3 Modeled ENMs Removal Efficiency

The modeled removal efficiency of different ENMs represents the percentage removal of ENMs by the CAS reactor under the four scenarios. The result shows 17 out of 17 kinds of ENMs have more than 50% removal from the CAS process under the general scenario. However, removal efficiency can be lower than 1% for SiO2-FITC. It means the removal efficiency of ENMs of the CAS process can be significantly different if ENMs have different characters. Characters of ENMs include but not limit to particle size, coating, zeta potential, surface charge and collision rate. However, no study has found quantitative relationships between ENMs properties and the removal efficiency of ENMs in WWTP until now.

Different studies conduct the ENMs experiments by using activated sludge at different concentration. Some studies use as low as 50 mg/L, and others use as high as 3,000 mg/L. From the database, it is clear that the concentration of activated sludge in the CAS reactor will affect the ENMs removal significantly. In general, higher biomass concentrations will lead to a higher removal of ENMs. With higher biomass concentration, there is increased possibility of classical colloidal interactions (i.e.

aggregation) and chemical interaction (i.e. sorption) to occur (Westerhoff, Kiser et al. 2013). However, ENMs removal efficiency and activated sludge concentration do not have a linear relationship, so it is impossible to predict ENMs removal efficiency under different activated sludge concentration without the model.

5.3.4 Relationship of Freundlich Isotherm Parameters and ENMs Removal Efficiency

Freundlich isotherm can represent the adsorption capability of different kinds of absorbates to absorbents. In this model, Freundlich isotherms are established for all ENMs. The model also predicts the ENMs removal efficiency based on the isotherms. Hence, Figure 13 shows the relationship of Freundlich adsorption capacity parameter, intensity parameter and ENMs removal efficiency under the general scenario.

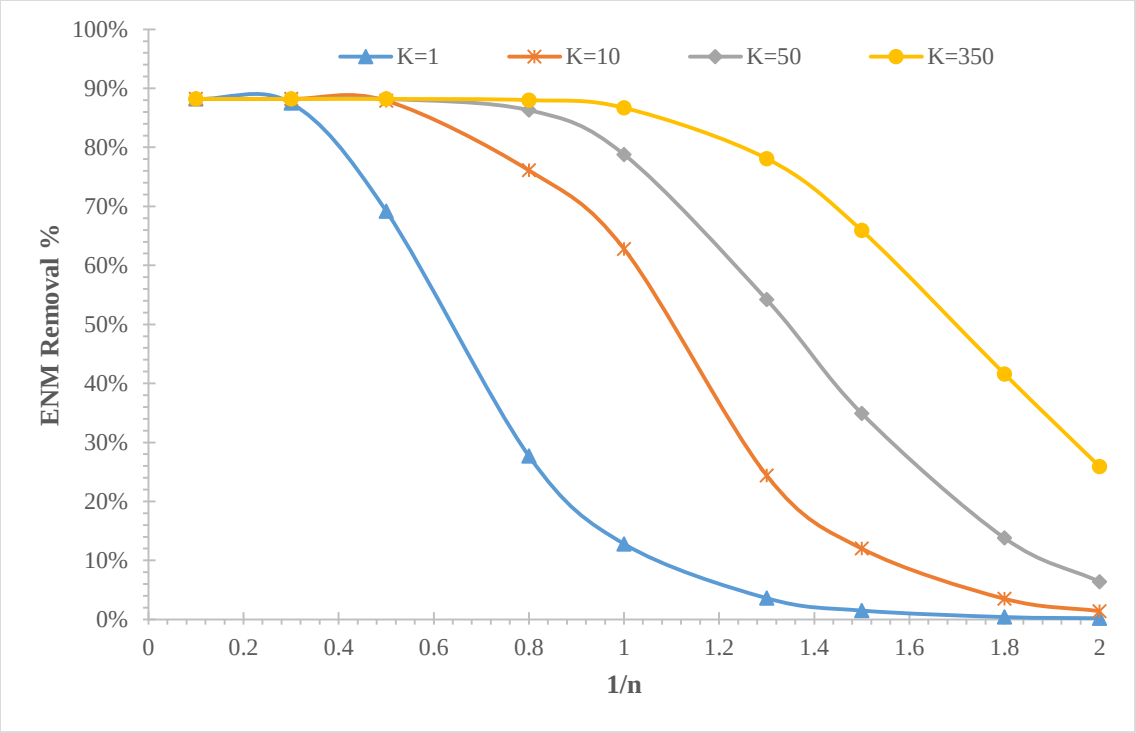

Figure 13. The relationship of Freundlich adsorption capacity parameter (K, (mg ENM/g biomass)(L/mg ENM)$^{1/n}$), intensity parameter (1/n, Unitless) and ENMs removal efficiency under general scenario (SRT=5d, COD=400 mg/L, C_0=10 µg/L)

When the adsorption capacity parameter (K) is the same, higher adsorption intensity parameter (1/n) means lower ENMs removal efficiency. Higher adsorption intensity parameter indicates unfavorable adsorption, and lower adsorption intensity parameter indicates favorable adsorption. It means unfavorable adsorption requires higher activated sludge concentration to reach ENMs removal than favorable adsorption. When the adsorption intensity parameter is the same, higher adsorption capacity means higher ENMs removal efficiency. Adsorption capacity indicates the capability of unit mass of absorbent to adsorb unit mass of absorbate, so ENMs with higher adsorption capacity requires less mass activated sludge to reach the same ENMs removal efficiency as the low adsorption capacity ones.

5.3.5 Kinetic Study of ENM Removal of the CAS Model

The CAS model is powerful when it comes to kinetic study of the CAS process. It is very convenient and can save researchers many time by running the program instead of running an experiment for a long time. It can predict the change of biomass concentration, and the change of ENM removal when changing the influent COD.

In this scenario, a kind of ENM is applied to the CAS model with determined adsorption capacity parameter (K) as 10 (mg ENM/g biomass)(L/mg ENM)$^{1/n}$, and the intensity parameter (1/n) as 1. The SRT is 5 days, and HRT is about 10 hours. The influent COD started at 1,000 mg/L, and then changed to 400 mg/L at day 60, then changed to 100 mg/L at day 220 and changed back to 400 mg/L at day 280. The influent ENM concentration started at 0.5 mg/L, and then changed to 0.05 mg/L at day 100. Figure 14 shows the change of biomass concentration had effluent ENM concentration under this scenario.

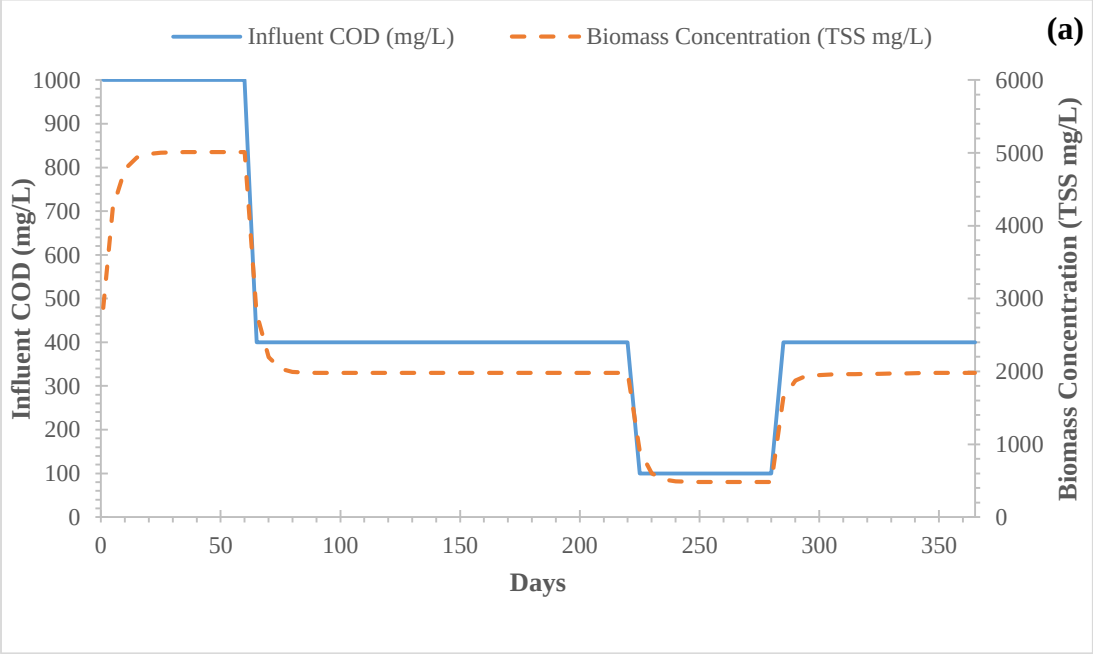

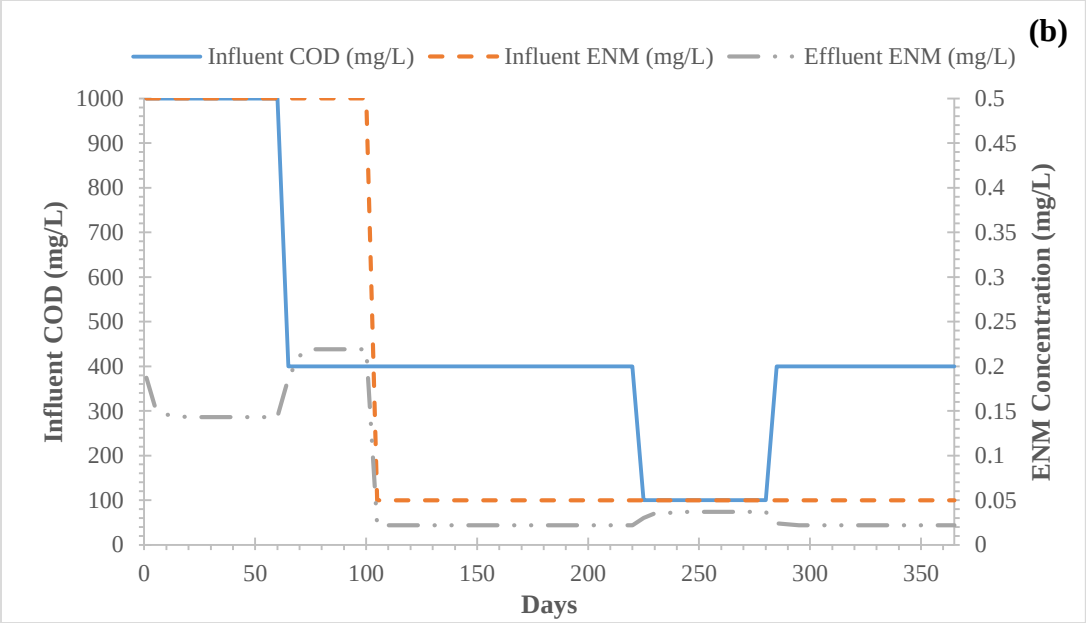

Figure 14. The kinetic study result of (a) change of biomass concentration, (b) effluent ENM concentration by the change of influent COD concentration and influent ENM concentration

The biomass concentration reached steady state after 10 days of change of influent COD. When the influent COD changed from 1,000 mg/L to 400 mg/L, the biomass concentration changed from 5,000 mg/L to 2,000 mg/L. When the influent COD changed from 400 mg/L to 100 mg/L, the biomass concentration changed from 2,000 mg/L to 500 mg/L. This shows the biomass concentration has positive correlation with influent COD.

The effluent ENM concentration decreases as the influent COD increases, because the biomass concentration increases as the influent COD increases. When influent COD changed from 1,000 mg/L to 400 mg/L at day 60, the effluent ENM concentration changed from 0.143 mg/L to 0.219 mg/L. Then the influent ENM changed from 0.5 mg/L to 0.05 mg/L at day 100, which caused the change of effluent ENM from 0.219 mg/L to 0.022 mg/L. Then the influent COD changed from 400 mg/L to 100 mg/L at day 220, the effluent ENM changed from 0.022 mg/L to 0.037 mg/L. Finally, when the influent COD changed from 100 mg/L to 400 mg/L at day 280, the effluent ENM concentration

changed from 0.037 mg/L to 0.022 mg/L. This result shows the influent COD have significant influence on the ENM removal rate.

5.4 Conclusion

Modeling result of effluent ENMs concentration of the CAS process showed 17 out of 33 ENMs have effluent concentration lower than 5 μg/L. Only 3 kinds of ENMs have effluent concentration higher than 9 μg/L. It showed that traditional WWTP process include the CAS process is able to removal many kinds of ENMs with high efficiency. The CAS model reached a steady state 30 days after changing influent COD from 400 mg/L to 1,000 mg/L. The change of model performance which include TSS and effluent COD happened mainly in the first 10 days. The removal of ENMs was related with TSS value of the CAS model.

The database summarized analytical work on quantifying ENMs removal by wastewater sludge. However, many studies are not nano-specific when it comes to quantifying ENMs concentration. The results of these studies also include particles which has larger diameter than nanoparticles, so the ENMs concentration should be lower than the results. Hence, it will affect the reliability of the ENMs removal efficiency by the CAS process. The model can only predict ENMs removal efficiency by the CAS process, which means it does not consider the attribution of other treatment process in the WWTP such as primary and tertiary treatment processes. The overall ENMs removal efficiency should increase if these treatment processes have been considered. Future works can input the data of ENMs removal by primary and tertiary treatment processes into the database.

CHAPTER 6

SUMMARY AND CONCLUSIONS

This chapter includes summary and conclusions of each chapter, followed by recommendations about future works.

The objective of chapter 3 is to quantitatively determine the removal of pristine and oxidized MWCNTs (O-MWCNTs) GO, and FLG from wastewater into the wastewater biomass. Results and conclusions of this chapter include:

• Quantification of GO and MWCNTs was determined by UV-Vis spectrophotometry, quantification of FLG was determined by programmable thermal analysis (PTA),

• At least 96% of pristine and O-MWCNTs were removed from the water phase through aggregation and 30-min settling in presence or absence of biomass with an initial MWCNT concentration of 25 mg/L.

• 65% of GO was removed with biomass concentration at or above 1,000 mg/L as total suspended solids (TSS) with the initial GO concentration of 25 mg/L.

•The removal of FLG at a biomass concentration of 50 mg TSS/L showed 16% removal of FLG with initial concentration of 1 mg/L. The current detection method limited the accessibility of using samples with higher biomass concentration.

•Majority of carbonaceous NMs entering into WWTPs would associate with biomass and be removed from the water phase.

The objective of chapter 4 is to quantitatively determine the removal of Tween™ 20 Ag ENM by wastewater biomass. The results and conclusions are:

•The removal efficiency of Tween™ 20 Ag ENM was from 11% to 92% at initial Ag ENM concentration from 970 μg/L to 2,600 μg/L with biomass concentration from 0.5 g/L to 3 g/L.

•WWTP with wastewater biomass concentration in the range of 2,000 mg/L to 5,000 mg/L can reach at least 50% removal of Tween™ 20 Ag ENM.

The objective of chapter 5 is to build a non-linear solids-to-liquid ratio distribution model to quantitatively evaluate the concentration of ENMs in the effluent of a CAS system based upon changes in influent COD, SRT, and initial ENMs concentration after primary sedimentation. The results and conclusions of this chapter are:

•Modeling result of effluent ENMs concentration of the CAS process shows 10 out of 17 ENMs have effluent concentration lower than 5 μg/L. Only 2 kinds of ENMs have effluent concentration higher than 9 μg/L.

•The change of TSS mostly happens in the first 10 days after the change of influent COD, then reaches a steady state with less than 5% fluctuation after day 11. The change of effluent COD happens mostly in the first 2 days, and reaches a steady state with less than 5% fluctuation from the third day.

•The CAS model can predict ENMs effluent concentration from the CAS process in different operational conditions, so it is adaptable to WWTPs in a wide range of operation circumstances. The database includes literature-reported experimental data of the removal efficiency of ENMs by wastewater, which can be the foundation of database of ENMs contamination in sewage through WWTP.

Future work can include quantitative study of the removal of other kinds of ENMs from WWTP by wastewater biomass if it is necessary to predict the removal of other kinds of ENMs by WWTP. Data of ENMs removal by primary and tertiary treatment in WWTP can be included in the database in order to present a comprehensive understanding of ENMs removal by WWTP. The result of the model can help companies to make decisions to meet the regulated emission standard of ENMs in the future.

REFERENCES

Ahamed, M., et al. (2008). "DNA damage response to different surface chemistry of silver nanoparticles in mammalian cells." Toxicology and Applied Pharmacology 233(3): 404-410.

Alkasrawi, M., et al. (2003). "The effect of Tween-20 on simultaneous saccharification and fermentation of softwood to ethanol." Enzyme and Microbial Technology 33(1): 71-78.

Alvarez, P. J. J., et al. (2009). "Research Priorities to Advance Eco-Responsible Nanotechnology." ACS Nano 3(7): 1616-1619.

APHA, et al. (2005). Standard Methods for the Examination of Water and Wastewater.

Ardern, E. and W. T. Lockett (1914). "Experiments on the oxidation of sewage without the aid of filters." Journal of the Society of Chemical Industry 33(10): 523-539.

Arepalli, S., et al. (2001). "Production and measurements of individual single-wall nanotubes and small ropes of carbon." Applied Physics Letters 78(11): 1610-1612.

Batteiger, B., et al. (1982). "The use of Tween 20 as a blocking agent in the immunological detection of proteins transferred to nitrocellulose membranes." Journal of immunological methods 55(3): 297-307.

Baur, J. and E. Silverman (2007). "Challenges and Opportunities in Multifunctional Nanocomposite Structures for Aerospace Applications." MRS Bulletin 32(04): 328-334.

Becker, W. C. and A. R. Foundation (2004). Using Oxidants to Enhance Filter Performance, AWWA Research Foundation and American Water Works Association.

Benn, T., et al. (2010). "The release of nanosilver from consumer products used in the home." Journal of environmental quality 39(6): 1875-1882.

Benn, T. M. and P. Westerhoff (2008). "Nanoparticle silver released into water from commercially available sock fabrics." Environ Sci Technol 42(11): 4133-4139.

Bhatt, I. and B. N. Tripathi (2011). "Interaction of engineered nanoparticles with various components of the environment and possible strategies for their risk assessment." Chemosphere 82(3): 308-317.

Brady-Estévez, A. S., et al. (2008). "A Single-Walled-Carbon-Nanotube Filter for Removal of Viral and Bacterial Pathogens." Small 4(4): 481-484.

Brar, S. K., et al. (2010). "Engineered nanoparticles in wastewater and wastewater sludge--evidence and impacts." Waste Manag 30(3): 504-520.

Bystrzejewska-Piotrowska, G., et al. (2009). "Nanoparticles: their potential toxicity, waste and environmental management." Waste Manag 29(9): 2587-2595.

Chen, K. L. and M. Elimelech (2009). "Relating colloidal stability of fullerene (C60) nanoparticles to nanoparticle charge and electrokinetic properties." Environ Sci Technol 43(19): 7270-7276.

Cho, H.-H., et al. (2011). "Effects of Solution Chemistry on the Adsorption of Ibuprofen and Triclosan onto Carbon Nanotubes." Langmuir 27(21): 12960-12967.

Cho, H.-H., et al. (2008). "Influence of Surface Oxides on the Adsorption of Naphthalene onto Multiwalled Carbon Nanotubes." Environ Sci Technol 42(8): 2899-2905.

Clark, S. and G. G. Mallick (2014). Global Graphene Market (Product Type, Application, Geography) - Size, Share, Global Trends, Company Profiles, Demand, Insights, Analysis, Research, Report, Opportunities, Segmentation and Forecast, 2013 - 2020, Allied Market Research. 2014.

Colvin, V. L. (2003). "The potential environmental impact of engineered nanomaterials." Nat Biotech 21(10): 1166-1170.

Doudrick, K., et al. (2013). "Extraction and quantification of carbon nanotubes in biological matrices with application to rat lung tissue." ACS Nano 7(10): 8849-8856.

Doudrick, K., et al. (2012). "Detection of Carbon Nanotubes in Environmental Matrices Using Programmed Thermal Analysis." Environmental Science & Technology 46(22): 12246-12253.

Doudrick, K., et al. (2015). "Quantification of graphene and graphene oxide in complex organic matrices." Environmental Science: Nano.

Drobne, D., et al. (2009). "In vivo screening to determine hazards of nanoparticles: nanosized TiO2." Environ Pollut 157(4): 1157-1164.

Fitts, J. P., et al. (2006). "Biotransformation of engineered nanoparticles in the environment." 2006 Philadelphia Annual Meeting.

Freundlich, H. (1906). "Concerning adsorption in solutions." Z. Phys. Chem. 57: 385–470.

Gartiser, S., et al. (2014). "Behavior of nanoscale titanium dioxide in laboratory wastewater treatment plants according to OECD 303 A." Chemosphere 104: 197-204.

George, T., et al. (2004). Wasterwater Engineering Treatment and Reuse, Mc GrawHill.

Gomez-Rivera, F., et al. (2012). "Fate of cerium dioxide (CeO2) nanoparticles in municipal wastewater during activated sludge treatment." Bioresour Technol 108: 300-304.

Gottschalk, F. and B. Nowack (2011). "The release of engineered nanomaterials to the environment." Journal of Environmental Monitoring 13(5): 1145-1155.

Gottschalk, F., et al. (2009). "Modeled Environmental Concentrations of Engineered Nanomaterials (TiO2, ZnO, Ag, CNT, Fullerenes) for Different Regions." Environ Sci Technol 43(24): 9216-9222.

Gottschalk, F., et al. (2013). "Environmental concentrations of engineered nanomaterials: review of modeling and analytical studies." Environ Pollut 181: 287-300.

Grady, J. L. C. P., et al. (1999). Biological Wastewater Treatment, CRC Press.

Handy, R. D., et al. (2012). "Ecotoxicity test methods for engineered nanomaterials: practical experiences and recommendations from the bench." Environ Toxicol Chem 31(1): 15-31.

He, H., et al. (1998). "A new structural model for graphite oxide." Chemical Physics Letters 287(1–2): 53-56.

Hendren, C. O., et al. (2011). "Estimating Production Data for Five Engineered Nanomaterials As a Basis for Exposure Assessment." Environ Sci Technol 45(7): 2562-2569.

Herrero-Latorre, C., et al. (2014). Characterization of carbon nanotubes and analytical methods for their determination in environmental and biological samples: A review.

Huang, H., et al. (2014). "Carbon nanotube composite membranes for small 'designer' water treatment systems." Water Science & Technology: Water Supply 14(5): 917.

Huang, T. S., et al. (2004). "Immobilization of antibodies and bacterial binding on nanodiamond and carbon nanotubes for biosensor applications." Diamond and Related Materials 13(4–8): 1098-1102.

Hyung, H. and J.-H. Kim (2008). "Natural Organic Matter (NOM) Adsorption to Multi-Walled Carbon Nanotubes: Effect of NOM Characteristics and Water Quality Parameters." Environ Sci Technol 42(12): 4416-4421.

Jarvie, H. P., et al. (2009). "Fate of Silica Nanoparticles in Simulated Primary Wastewater Treatment." Environ Sci Technol 43(22): 8622-8628.

Kaegi, R., et al. (2011). "Behavior of metallic silver nanoparticles in a pilot wastewater treatment plant." Environ Sci Technol 45(9): 3902-3908.

Keller, A. A. and A. Lazareva (2014). "Predicted Releases of Engineered Nanomaterials: From Global to Regional to Local." Environmental Science & Technology Letters 1(1): 65-70.

Kim, B., et al. (2010). "Discovery and Characterization of Silver Sulfide Nanoparticles in Final Sewage Sludge Products." Environ Sci Technol 44(19): 7509-7514.

Kim, J. S., et al. (2007). "Antimicrobial effects of silver nanoparticles." Nanomedicine 3(1): 95-101.

Kiser, M. A. (2011). Fate of Engineered Nanomaterials in Wastewater Treatment Plants. Ann Arbor, Arizona State University. 3487335: 257.

Kiser, M. A., et al. (2012). "Nanomaterial transformation and association with fresh and freeze-dried wastewater activated sludge: implications for testing protocol and environmental fate." Environ Sci Technol 46(13): 7046-7053.

Kiser, M. A., et al. (2010). "Quantitatively Understanding the Performance of Membrane Bioreactors." Separation Science and Technology 45(7): 1003-1013.

Kiser, M. A., et al. (2010). "Biosorption of nanoparticles to heterotrophic wastewater biomass." Water Research 44(14): 4105-4114.

Kiser, M. A., et al. (2009). "Titanium nanomaterial removal and release from wastewater treatment plants." Environ Sci Technol 43(17): 6757-6763.

Klaine, S. J., et al. (2008). "Nanomaterials in the environment: behavior, fate, bioavailability, and effects." Environ Toxicol Chem 27(9): 1825-1851.

Klaine, S. J., et al. (2012). "Paradigms to assess the environmental impact of manufactured nanomaterials." Environmental Toxicology and Chemistry 31(1): 3-14.

Kloepfer, J. A., et al. (2005). "Uptake of CdSe and CdSe/ZnS Quantum Dots into Bacteria via Purine-Dependent Mechanisms." Applied and Environmental Microbiology 71(5): 2548-2557.

Kvitek, L., et al. (2009). "Initial Study on the Toxicity of Silver Nanoparticles (NPs) against Paramecium caudatum." The Journal of Physical Chemistry C 113(11): 4296-4300.

Laspidou, C. S. and B. E. Rittmann (2002). "Non-steady state modeling of extracellular polymeric substances, soluble microbial products, and active and inert biomass." Water Res 36(8): 1983-1992.

Limbach, L. K., et al. (2008). "Removal of oxide nanoparticles in a model wastewater treatment plant: influence of agglomeration and surfactants on clearing efficiency." Environ Sci Technol 42(15): 5828-5833.

Ma, X., et al. (2010). "Interactions between engineered nanoparticles (ENPs) and plants: phytotoxicity, uptake and accumulation." Sci Total Environ 408(16): 3053-3061.

Mangematin, V. and S. Walsh (2012). "The future of nanotechnologies." Technovation 32(3–4): 157-160.

Mitrano, D. M., et al. (2012). "Detecting nanoparticulate silver using single-particle inductively coupled plasma–mass spectrometry." Environmental Toxicology and Chemistry 31(1): 115-121.

Monod, J. (1950). "{L}a technique de culture continue, theorie et applications." {A}nnales d'{I}nstitute {P}asteur 79: 390-410.

Moore, M. N. (2006). "Do nanoparticles present ecotoxicological risks for the health of the aquatic environment?" Environ Int 32(8): 967-976.

Mueller, N. C. and B. Nowack (2008). "Exposure modeling of engineered nanoparticles in the environment." Environmental Science and Technology 42(12): 4447-4453.

Neidhardt, F. C., Ed. (1996). Escherichia coli and Salmonella: Cellular and Molecular Biology. , ASM Press.

Nowack, B. and T. D. Bucheli (2007). "Occurrence, behavior and effects of nanoparticles in the environment." Environ Pollut 150(1): 5-22.

Nowack, B., et al. (2013). "Potential release scenarios for carbon nanotubes used in composites." Environ Int 59: 1-11.

Nowack, B., et al. (2012). "Potential scenarios for nanomaterial release and subsequent alteration in the environment." Environmental Toxicology and Chemistry 31(1): 50-59.

Panáček, A., et al. (2009). "Antifungal activity of silver nanoparticles against Candida spp." Biomaterials 30(31): 6333-6340.

Peralta-Videa, J. R., et al. (2011). "Nanomaterials and the environment: A review for the biennium 2008-2010." J Hazard Mater 186(1): 1-15.

Petersen, E. J., et al. (2011). "Potential Release Pathways, Environmental Fate, And Ecological Risks of Carbon Nanotubes." Environmental Science & Technology 45(23): 9837-9856.

Piccinno, F., et al. (2012). "Industrial production quantities and uses of ten engineered nanomaterials in Europe and the world." Journal of Nanoparticle Research C7 - 1109 14(9): 1-11.

Plata, D. L., et al. (2012). "Thermogravimetry-Mass Spectrometry for Carbon Nanotube Detection in Complex Mixtures." Environ Sci Technol 46(22): 12254-12261.

Rottman, J., et al. (2012). "Interactions of inorganic oxide nanoparticles with sewage biosolids." Water Sci Technol 66(9): 1821-1827.

Saleh, N. B., et al. (2008). "Aggregation Kinetics of Multiwalled Carbon Nanotubes in Aquatic Systems: Measurements and Environmental Implications." Environ Sci Technol 42(21): 7963-7969.

Seabra, A. B., et al. (2014). "Nanotoxicity of Graphene and Graphene Oxide." Chemical Research in Toxicology 27(2): 159-168.

Shin, H.-J., et al. (2009). "Efficient Reduction of Graphite Oxide by Sodium Borohydride and Its Effect on Electrical Conductance." Advanced Functional Materials 19(12): 1987-1992.

Smith, B., et al. (2009). "Influence of Surface Oxides on the Colloidal Stability of Multi-Walled Carbon Nanotubes: A Structure−Property Relationship." Langmuir 25(17): 9767-9776.

Stankus, D. P., et al. (2011). "Interactions between Natural Organic Matter and Gold Nanoparticles Stabilized with Different Organic Capping Agents." Environ Sci Technol 45(8): 3238-3244.

Suzuki, K., et al. (2002). "Removal of phosphate, magnesium and calcium from swine wastewater through crystallization enhanced by aeration." Water Res 36(12): 2991-2998.

U.S.EPA (2010). Interim Technical Guidance for Assessing Screening Level Environmental Fate and Transport of, and General Population, Consumer, and Environmental Exposure to Nanomaterials Washington, DC, Office of Pollution Prevention and Toxics (OPPT), U.S. Environmental Protection Agency.

U.S.EPA (2013). Comprehensive Environmental Assessment Applied to Multiwalled Carbon Nanotube Flame-Retardant Coatings in Upholstery Textiles: A Case Study Presenting Priority Research Gaps for Future Risk Assessments (Final Report). Washington, DC, U.S. Environmental Protection Agency. EPA/600/R-12/043F.

Upadhyayula, V. K. K., et al. (2009). "Application of carbon nanotube technology for removal of contaminants in drinking water: A review." Science of The Total Environment 408(1): 1-13.

von der Kammer, F., et al. (2012). "Analysis of engineered nanomaterials in complex matrices (environment and biota): general considerations and conceptual case studies." Environ Toxicol Chem 31(1): 32-49.

Wang, C., et al. (2013). "Removal of aqueous fullerene nC60 from wastewater by alum-enhanced primary treatment." Separation and Purification Technology 116: 61-66.

Wang, Y., et al. (2012). "Fate and biological effects of silver, titanium dioxide, and C60 (fullerene) nanomaterials during simulated wastewater treatment processes." J Hazard Mater 201-202: 16-22.

Westerhoff, P. and B. Nowack (2013). "Searching for Global Descriptors of Engineered Nanomaterial Fate and Transport in the Environment." Accounts of Chemical Research 46(3): 844-853.

Westerhoff, P., et al. (2011). "Occurrence and removal of titanium at full scale wastewater treatment plants: implications for TiO2 nanomaterials." J Environ Monit 13(5): 1195-1203.

Westerhoff, P. K., et al. (2013). "Nanomaterial Removal and Transformation During Biological Wastewater Treatment." Environmental Engineering Science 30(3): 109-117.

Wiesner, M. R. and J.-Y. Bottero (2011). "A risk forecasting process for nanostructured materials, and nanomanufacturing." Comptes Rendus Physique 12(7): 659-668.

Wiesner, M. R., et al. (2009). "Decreasing uncertainties in assessing environmental exposure, risk, and ecological implications of nanomaterials." Environ Sci Technol 43(17): 6458-6462.

Xiao, S., et al. (2009). "Immobilization of Zerovalent Iron Nanoparticles into Electrospun Polymer Nanofibers: Synthesis, Characterization, and Potential Environmental Applications." The Journal of Physical Chemistry C 113(42): 18062-18068.

Yang, S.-T., et al. (2010). "Folding/aggregation of graphene oxide and its application in Cu 2+ removal." Journal of Colloid and Interface Science 351(1): 122-127.

Yang, Y., et al. (2012). "Potential nanosilver impact on anaerobic digestion at moderate silver concentrations." Water Research 46(4): 1176-1184.

Yang, Y., et al. (2014). "Simultaneous removal of nanosilver and fullerene in sequencing batch reactors for biological wastewater treatment." Chemosphere.

Yang, Y., et al. (2015). "Interaction of Carbonaceous Nanomaterials with Wastewater Biomass." Frontiers of Environmental Science and Engineering.

Yi, P. and K. L. Chen (2011). "Influence of Surface Oxidation on the Aggregation and Deposition Kinetics of Multiwalled Carbon Nanotubes in Monovalent and Divalent Electrolytes." Langmuir 27(7): 3588-3599.

Zhang, J., et al. (2010). "Reduction of graphene oxide vial-ascorbic acid." Chemical Communications 46(7): 1112-1114.

APPENDIX A

THE ESTABLISHMENT OF DATABASE OF PARAMETERS OF THE NON-LINEAR SOLID TO LIQUID DISTRIBUTION OF ENM

The parameters of the non-linear solid to liquid distribution of ENMs are critical for the model to predict the effluent ENM concentration. The parameters include capacity parameter (K) and intensity parameter (1/n). Each kind of ENMs in the database has unique parameters to represent the characteristic of solid to liquid distribution. Some published papers have included determined parameters of ENMs, so the parameters are included in the database. Others do not have the parameters, so the data of the removal efficiency, biomass concentration and initial ENMs concentration are included in Table 8, then isotherms are built based on these data.

Table 8. Removal efficiency of ENMs by different concentration of biomass, with different initial concentration of ENMs.

ENM	Experiment ENM concentration (mg/L)	removal %	Experiment Biomass Concentration (g/L)	Have Isotherm in Original Paper	Reference
AgNP(A)	0.06 to 0.49	99	N/A	Yes	Benn et al. 2007
CeO2(A)	100	95±1	3	No	Limbach et al. 2008
SiO2(A)	2470	99	0.293	No	Jarvie et al. 2009
TiO2(A)	0.1 to 3	99.9	N/A	Yes	Kiser et al. 2009
SiO2-FITC	1 to 50	21±4	0.4	Yes	Kiser et al. 2010
AgNP(B)	0.6	96±1	0.05	No	Kiser et al. 2010
aq-nC60(A)	4	88±8	0.4	No	Kiser et al. 2010
f-Ag	0.5	38±2	0.4	No	Kiser et al. 2010
fn-Ag	0.5 to 1.5	88±4	1.8±0.2	No	Wang et al. 2011
TiO2(B)	0.5 to 2.0	97±1	1.3±0.2	No	Wang et al. 2011
C60(A)	1.8 to 2.2	96	2±0.2	No	Wang et al. 2011
AgNP(C)	0.13 to 2.4	95	3	No	Kaegi et al. 2011
PVA-AgNP	40	91	3	No	Yang et al. 2011
TiO2(C)	0.18 to 1.23	98.3	2	No	Westerhoff et al. 2011
CeO2(B)	55	98.5	0.248±0.05	No	Gomez-Rivera et al. 2012
Car-Ag	2.1±0.05	60±4	0.8	No	Kiser et al. 2012
Cit-Ag	0.4	38	0.8	No	Kiser et al. 2012
PVP-Ag	0.1	48	0.8	No	Kiser et al. 2012

ENM	Experiment ENM concentration (mg/L)	removal %	Experiment Biomass Concentration (g/L)	Have Isotherm in Original Paper	Reference
GA-Ag	0.5	62	0.8	No	Kiser et al. 2012
TA-Au	2.2±0.3	90±2	0.8	No	Kiser et al. 2012
PVP-Au	0.9	52±25	0.8	No	Kiser et al. 2012
Car-PS	2	91±1	0.8	No	Kiser et al. 2012
Sulf-PS	2	92±2	0.8	No	Kiser et al. 2012
aq-nC60(B)	3.4±0.04	92±1	0.8	No	Kiser et al. 2012
Al2O3	0.5 to 200	73.4	N/A	Yes	Rottman et al. 2012
CeO2(C)	0.5 to 200	82.5	N/A	Yes	Rottman et al. 2012
SiO2(B)	0.5 to 200	27.7	N/A	Yes	Rottman et al. 2012
C60(B)	0.2	96	0.279±0.025	No	Wang et al. 2013
TiO2-P25	1 to 10	95	2	No	Gartiser et al. 2013
FLG	1	72.2	2	Yes	Yang et al. 2015
GO	25	94.2	2	Yes	Yang et al. 2015
nC60	0.07 to 2	99.5	2	Yes	Yang et al. 2015
Tween-20 Ag	0.97 to 2.6	99.9	2	Yes	Original

For the ENMs which do not have isotherm in the original paper, isotherms were made based upon the removal rate, initial ENM concentration and biomass concentration. All isotherms were included in Figure 15.

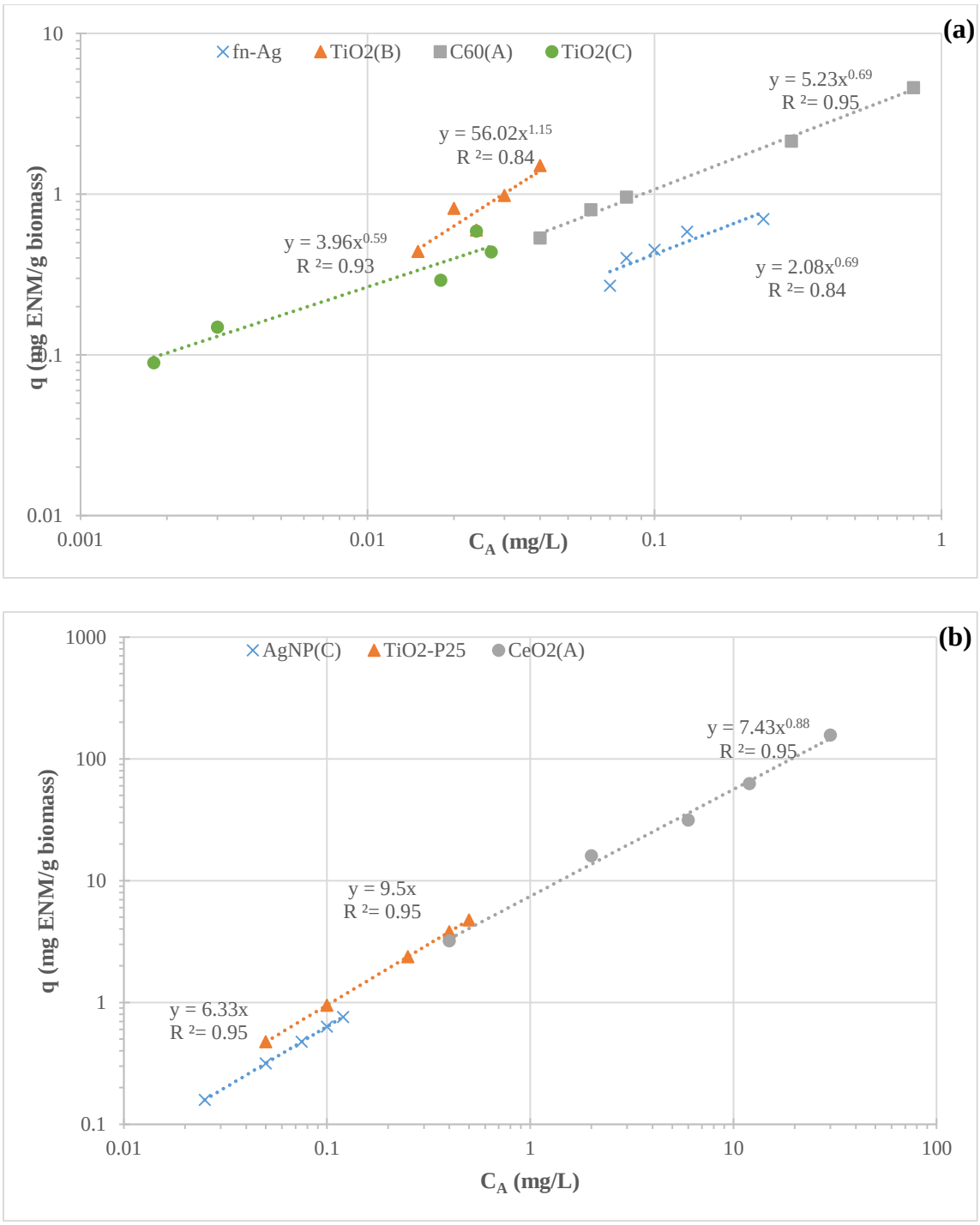

Figure 15. ENM non-linear solid to liquid distribution isotherms

APPENDIX B

MASS BALANCE OF ENM OF THE CAS MODEL

In order to get the result of the model, the iteration start with an initial value X_0. To prove the iteration process is able to get the final result of effluent ENM concentration, the iteration process of ENM is illustrated here.

For TiO_2 (A), the adsorption capacity parameter (K) is 34.32 (mg ENM/g biomass)(L/mg ENM)$^{1/n}$, the intensity parameter (1/n) is 0.48. The model is under general scenario, which means SRT is 5 days, influent COD is 400 mg/L. Biomass concentration in the effluent is 0.02 g/L, and is 10 g/L in the waste stream. The initial ENM concentration C_0 is 1 mg/L. The influent flow rate (Q_0) is 8.67×10^8 L, the effluent flow rate (Q_{eff}) is 8.54×10^8 L, the waste stream flowrate (Q_{was}) is 1.3×10^7 L. Set the initial value of X_0 as $0.1C_0$, the iteration result is shown as Table 9.

Table 9. Iteration result of CAS model with initial value of $0.1C_0$

Iteration #	M_0 (mg/d)	C_{eff} (mg/L)	M_{eff} (mg/d)	M_{was} (mg/d)	Difference of Mass Balance
1	8.67×10^8	0.0002	1.00×10^7	7.44×10^7	90%
2	8.67×10^8	0.0041	4.54×10^7	3.17×10^8	58%
3	8.67×10^8	0.0159	9.38×10^7	6.08×10^8	19%
4	8.67×10^8	0.0235	1.17×10^8	7.34×10^8	2%
5	8.67×10^8	0.0244	1.19×10^8	7.47×10^8	0%
6	8.67×10^8	0.0244	1.19×10^8	7.47×10^8	0%

M_0 is the mass of ENM in the influent, M_{eff} and M_{was} are mass of ENM in the effluent and waste stream, respectively. Q_{was} is the waste stream flow rate. The difference of mass balance is $(M_0-M_{eff}-M_{was})/M_0$,which means the difference of Eq (5.4) on both side. Smaller difference means the model result is closer to mass balance. Table n. shows the iteration took six steps to get the result of the model, which have no difference between each side of Eq (5.4).

Initial value X_0 is critical for the iteration, it determines the number of steps that are needed for the iteration process to find an answer. If the X_0 value changes from $0.1C_0$ to $0.01\ C_0$, the iteration result is shown as Table 10. The iteration took three steps to get the result of the model. There is no difference between each side of the mass balance, so the result can represent the effluent ENM concentration.

Table 10. Iteration result of CAS model with initial value of $0.01C_0$

Iteration #	M_0 (mg/d)	C_{eff} (mg/L)	M_{eff} (mg/d)	M_{was} (mg/d)	Difference of Mass Balance
1	8.67×10^8	0.02	1.07×10^8	6.79×10^8	9%
2	8.67×10^8	0.0242	1.19×10^8	7.44×10^8	0%
3	8.67×10^8	0.0244	1.19×10^8	7.47×10^8	0%

APPENDIX C

FORTRAN CODES FOR CONVENTIONAL ACTIVATED SLUDGE MODEL

The FORTRAN codes include CAS model input parameters and CAS model main code. The CAS model is built and optimized bases upon previous paper. The codes that are bolded are elements created or modified for optimization of different scenarios.

CAS Model Input Parameters

$CASfparam

```
 Q0     = 867000000.0,
 S0     = 400.0,
 Xa0    = 0.0,
 Xres0  = 50.0,
 EPS0   = 0.0,
 UAP0   = 0.0,
 BAPS0  = 0.0,
 BAPL0  = 0.0,
 O20    = 3.0,

 C0     = 0.05
 X0     = 0.001
 Kad    = 10
 a      = 1

 qS       = 10.0,
 qD       = 1.5,
 qBAP     = 0.07,
 qUAP     = 1.27,
 YS       = 0.4,
 YP       = 0.45,
 KBAP     = 85.0,
 KS       = 10.0,
 KD       = 0.8,
 KUAP     = 100.0,
 KO       = 0.5,
 b        = 0.1,
 fd       = 0.8,
 k1       = 0.05,
 kEPS     = 0.18,
 khyd     = 0.17,
 xBAPS    = 0.35,
 kLa      = 2000.0,
```

V = 370000000,
d = 5.0,
thetax = 5.0,
e = 0.8,

Xv_eff = 20,
Xv_rec = 10000,

Si = 10.0,
Xai = 2000.0,
Xresi = 100.0,
EPSi = 100.0,
UAPi = 1.0,
BAPSi = 50.0,
BAPLi = 50.0,
O2i = 3.0,
Qwi = 12700,

SOTE = 2.0,
c1s = 8.7,
c1 = 2.0,
beta = 0.95,
T = 25.0,

Ci0 = 0.5,
kb = 9000,
Kp = 0.00006,
Hc = 0.000265,
kLac = 0.1,
xsur = 0.33,
p1 = 1.00,
n_air = 0.28,
R = 8.31,
R_dry = 287.05,

ts = 1.0,
tdmax = 100,

$end

The CAS Model

PROGRAM CASf

IMPLICIT REAL*8 (a-h,o-z)

REAL*8 Q0,S0,Xa0,Xres0,EPS0,UAP0,BAPS0,BAPL0,ISS,O20, &
qS,qBAP,qUAP,YS,YP,KBAP,KS,KUAP,b,fd,k1,kEPS,khyd,xBAPS, &
V,d,thetax,e, &
Si,Xai,Xresi,EPSi,UAPi,BAPSi,BAPLi,O2i,Qwi, &
ts,td,tdmax, &

S_old,Xa_old,Xres_old,EPS_old,UAP_old,BAPS_old,BAPL_old,Xv_old,Qw_old,Qe_old, &

S_new,Xa_new,Xres_new,EPS_new,UAP_new,BAPS_new,BAPL_new,Xv_new,Qw_new,Qe_new, &
rs,BAP, &

thetad,thetah, &
Xv,Xv_eff,Xv_rec,XvSS,Xratio, &
Xv_is,y_theta,X,XSS,Xg,Xkg, &
dXa_dt,dXv_dt,dXSS_dt,dXSS_dt_kg,dXv_dt_biol, &
SWR, &
N,P, &
EffProd,WastProd, &
EQ_COD,EQ_BODL,EQ_BOD5,COD_sum,COD_loading, Rem_COD, &
O2input,O2output,O2uptake,O2uptake_kg, &
SOTE,c1s,c1,beta,T,alpha_KK,FOTE_KK,alpha_C,FOTE_C, &
Power_KK,Power_C, &

Ci0,kb,kb_mg,Kp,Kp_mg,kLac,xsur,Hc,Hc_LL,p1,p2,n_air,R,R_dry,w,Qa, &

```
Qa_L,rho_air,Ci,Rem_Ci,Mass_inf,Mass_eff,Mass_was,Mass_vol,Mass_aer,Mass_sor,M
ass_bio, &
      Ci_eff,Ci_was,Ci_vol,Ci_aer,Ci_sor,Ci_bio,Ci_sum, &
      total_time, &

      Qe,Qw,C0,Ce,Xa_eff,Xa_rec,Kad,a,epsilon,x0,x1

REAL*4 t0,KD,KO,kLa
INTEGER nt,i

NAMELIST/CASfparam/ &
       Q0,S0,Xa0,Xres0,EPS0,UAP0,BAPS0,BAPL0,O20, &

qS,qD,qBAP,qUAP,YS,YP,KBAP,KS,KD,KUAP,KO,b,fd,k1,kEPS,khyd,xBAPS,kLa, &
       V,d,thetax,e, &
          Xv_eff,Xv_rec, &
       Si,Xai,Xresi,EPSi,UAPi,BAPSi,BAPLi,O2i,Qwi, &
          SOTE,c1s,c1,beta,T, &
          Ci0,kb,Kp,Hc,kLac,xsur,p1,n_air,R,R_dry, &
       ts,tdmax, &
       C0,X0,Kad,a,Xvad


! Start counting runtime
t0 = SECNDS(0.0)


! Read input file
OPEN(unit=1, file='CASfparam.in', status='old')
READ(unit=1, nml=CASfparam)
CLOSE(1)


! Derived parameters
Xres0 = 0.08*S0
ISS   = 0.05*S0


! Time stepping
td    = ts / (60*60*24)   ! size of time step in days
nt    = tdmax / td        ! total number of time steps


! Initialize time-dependent quantities
```

```
S_old    = Si
Xa_old   = Xai
Xres_old = Xresi
EPS_old  = EPSi
UAP_old  = UAPi
BAPS_old = BAPSi
BAPL_old = BAPLi
O2_old   = O2i
Qw_old           = Qwi

! Iteration criterion
epsilon = 0.01

!!!!!!!!!!!!!!!!!!!!!!!!!!!!!!!!!!!!!!!!!!!!!!!!!!!!!!!!!!!
! Do the time integration of the differential equations !
!!!!!!!!!!!!!!!!!!!!!!!!!!!!!!!!!!!!!!!!!!!!!!!!!!!!!!!!!!!


DO i=1,nt

  rs       = qS*S_old/(KS+S_old)
  BAP      = BAPS_old + BAPL_old
  Xv_old   = Xa_old + Xres_old + EPS_old
  Qe_old   = Q0 - Qw_old

  S_new    = S_old + ( -rs*Xa_old + Q0*S0/V - Qe_old*S_old/V - Qw_old*S_old/V ) *
td
  Xa_new   = Xa_old + ( YS*rs*(1-k1-kEPS)*Xa_old +
YP*(qUAP*UAP_old/(KUAP+UAP_old) + qBAP*BAP/(KBAP+BAP))*Xa_old -
b*Xa_old + &
   Q0*Xa0/V - Qe_old*(Xa_old*Xv_eff/Xv_old)/V -
Qw_old*(Xa_old*Xv_rec/Xv_old)/V) * td
  Xres_new = Xres_old + ( b*(1-fd)*Xa_old + Q0*Xres0/V -
Qe_old*(Xres_old*Xv_eff/Xv_old)/V - Qw_old*(Xres_old*Xv_rec/Xv_old)/V) * td
  EPS_new  = EPS_old + ( kEPS*rs*Xa_old - khyd*EPS_old + Q0*EPS0/V - &
   Qe_old*(EPS_old*Xv_eff/Xv_old)/V - Qw_old*(EPS_old*Xv_rec/Xv_old)/V) * td
  UAP_new  = UAP_old + ( k1*rs*Xa_old -
Xa_old*qUAP*UAP_old/(KUAP+UAP_old) + Q0*UAP0/V - Qe_old*UAP_old/V -
Qw_old*UAP_old/V ) * td
  BAPS_new = BAPS_old + ( xBAPS*khyd*EPS_old -
Xa_old*qBAP*BAPS_old/(KBAP+BAPS_old) &
   + Q0*BAPS0/V - Qe_old*BAPS_old/V - Qw_old*BAPS_old/V ) * td
  BAPL_new = BAPL_old + ( (1-xBAPS)*khyd*EPS_old -
Xa_old*qBAP*BAPL_old/(KBAP+BAPL_old) &
   + Q0*BAPL0/V - Qe_old*BAPL_old/V - Qw_old*BAPL_old/V ) * td
```

```
  Xv_new   = Xa_new + Xres_new + EPS_new
  Qw_new   = (Xa_old*V -
thetax*Qe_old*Xa_old*Xv_eff/Xv_old)/(thetax*Xa_old*Xv_rec/Xv_old)
  Qe_new   = Q0-Qw_new

  S_old    = S_new
  Xa_old   = Xa_new
  Xres_old = Xres_new
  EPS_old  = EPS_new
  UAP_old  = UAP_new
  BAPS_old = BAPS_new
  BAPL_old = BAPL_new
  Xv_old   = Xv_new
  Qw_old   = Qw_new
  Qe_old   = Qe_new

ENDDO

DO
  x1=x0-(((Q0*C0 - (Kad*x0**(a))*(0.001*Xv_eff*Qe_new +
0.001*Xv_rec*Qw_new))/(Qe_new + Qw_new)-x0)/&
  ((((-Kad)*(0.001*Xv_eff*Qe_new + 0.001*Xv_rec*Qw_new)*a*x0**(a-
1)))/(Qe_new + Qw_new)-1))

write(6,*) "Root = ", x1

if (abs (x1-x0)/x0 < epsilon ) exit

   x0=x1

END DO

!!!!!!!!!!!!!!!!!!!!!!!!!!!!!!!!
! Calculate final output values !
!!!!!!!!!!!!!!!!!!!!!!!!!!!!!!!!


! System Hydraulic Detention Time
thetad = V/Q0         ! days
thetah = thetad*24    ! hours


! Mixed Liquor Volatile Suspended Solids, MLVSS
Xv   = Xv_new           ! mg CODX/L
XvSS = Xv/1.42  ! mg VSS/L
```

```
! Ratio of Active to Volatile Suspended Solids
Xratio = Xa_new/Xv


! Estimation of Mixed Liquor Suspended Solids, MLSS
Xv_is   = Xv * 10/90            ! Inorganic solids of MLVSS (assuming 10 parts inorganics
per 90 parts organics) (mg COD_X/L)
y_theta = ISS*thetax/thetad       ! Input inorganic suspended solids (mg COD_X/L)
X       = Xv + Xv_is + y_theta    ! mg COD_X/L
XSS     = X / (0.9*1.42)          ! mg SS/L
Xg      = X / (1000*1.42*0.9)     ! g SS_X/L (assuming VSS = 0.9SS)
Xkg     = Xg / 1000               ! kg SS_X/L


! Effluent and Recycle Components
Xa_eff   = Xa_new*(Xv_eff/Xv)
Xres_eff = Xa_new*(Xv_eff/Xv)
EPS_eff  = EPS_new*(Xv_eff/Xv)
Xa_rec   = Xa_new*(Xv_rec/Xv)
Xres_rec = Xres_new*(Xv_rec/Xv)
EPS_rec  = EPS_new*(Xv_rec/Xv)


! Solids Loss Rate
dXa_dt      = Xa_new * V/thetax           ! mg COD_X/d
dXv_dt      = Xv * V/thetax             ! mg COD_X/d
dXSS_dt     = X * V/thetax                ! mg COD_X/d
dXSS_dt_kg  = dXSS_dt / 1000000       ! kg COD_X/d
dXv_dt_biol = dXv_dt - Q0*Xres0       ! mg COD_X/d


! Sludge Wasting Rate
SWR = Qw_new*X*(Xv_rec/Xv)/1000000    ! kg COD_X/d


! Nutrient Requirements
N = dXv_dt_biol * 0.124/Q0    ! mg N/L
P = dXv_dt_biol * 0.025/Q0    ! mg P/L


! Effluent and Wasted EPS, UAP, and BAP
EffProd  = (EPS_new*Xv_eff/Xv) + UAP_new + BAPS_new + BAPL_new      ! mg
COD_P/L
```

```
WastProd = (EPS_new*Xv_eff/Xv) + UAP_new + BAPS_new + BAPL_new    ! mg
COD_P/L


! Effluent Quality
EQ_COD      = ISS+ S_new + Xv_eff + UAP_new + BAPS_new + BAPL_new    ! mg
COD/L
EQ_BODL     = S_new + Xa_eff + UAP_new + BAPS_new + BAPL_new! mg
BOD_L/L
EQ_BOD5     = 0.68*S_new + 0.14*(UAP_new + BAPS_new)                 ! mg
BOD_5/L
COD_sum     = S0+Xa0+Xres0+EPS0+UAP0+BAPS0+BAPL0+ISS                 ! mg
COD/L
COD_loading = Q0*COD_sum/(1000*V)                                    !
kg/m^3/d
Rem_COD     = (1-(EQ_COD/COD_sum))*100                               ! %


! Oxygen Supply Rate Needed
O2input     = Q0*(O20+COD_sum-ISS)                                   ! mg
02/d
O2output    = Qe_new*(S_new+Xv_eff+UAP_new+BAPS_new+BAPL_new) +
Qw_new*(S_new+Xv_rec+UAP_new+BAPS_new+BAPL_new)          ! mg 02/d
O2uptake    = O2input - O2output                                     ! mg O2/d
O2uptake_kg = O2uptake / 1000000                                     ! kg
O2/d


! Field Oxygen Transfer Efficiency
alpha_KK = EXP(-0.08788*Xg)                                          ! kg O2/kWh
FOTE_KK  = SOTE * 1.035**(T-20) * alpha_KK * (beta*c1s-c1) / 9.2     ! kg O2/kWh
alpha_C  = EXP(-0.046*Xg)                                            ! kg O2/kWh
FOTE_C   = SOTE * 1.035**(T-20) * alpha_C * (beta*c1s-c1) / 9.2      ! kg O2/kWh


! Power Required for Aeration
Power_KK = O2uptake_kg / (FOTE_KK*24)    ! kW
Power_C  = O2uptake_kg / (FOTE_C*24)     ! kW


! Pollutant Fate
Hc_LL            = Hc/(0.082054*293/1000)                            ! L
water/L gas
Kp_mg            = Kp/(0.9*1000*1.42)                                ! L/mg
COD_P
```

```
kb_mg     = kb/(0.9*1000*1.42)                                    ! L/mg COD_P-d
p2        = ((p1*101330)+(1000*9.8*d))/101330                     ! atm
w         = (29.7*n_air*e*Power_KK)/(R*T*(((p2/p1)**0.283)-1))          ! kg air/s
rho_air   = (p1*101330)/(R_dry*(T+273))                           ! kg/m^3
Qa        = (w/rho_air)*86400                                             !m^3/d
Qa_L      = Qa*1000                                                       !L/d
Ci        =
(Q0*Ci0)/(Qe_new+Qw_new+(xsur*kLac*V)+(Qa_L*Hc_LL)+(Xv_rec*Kp_mg*Qw_n
ew+Xv_eff*Kp_mg*Qe_new)+(kb_mg*Xa_new*V))        !mg Ci/L
Rem_Ci    = (1-(Ci/Ci0))*100                                      ! %
Mass_inf  = Q0*Ci0                                                ! mg Ci/d
Mass_eff  = Qe_new*Ci                                             ! mg Ci/d
Mass_was  = Qw_new*Ci                                             ! mg Ci/d
Mass_vol  = (kLac*xsur*V*Ci)                                      ! mg Ci/d
Mass_aer  = Qa_L*Hc_LL*Ci                                         ! mg Ci/d
Mass_sor  = Xv_rec*Ci*Kp_mg*Qw_new+Xv_eff*Ci*Kp_mg*Qe_new         !mg
Ci/d
Mass_bio  = kb_mg*Xa_new*Ci*V                                     !mg Ci/d
Ci_eff    = (Mass_eff/Mass_inf)*100                               ! %
Ci_was    = (Mass_was/Mass_inf)*100                               ! %
Ci_vol    = (Mass_vol/Mass_inf)*100                               ! %
Ci_aer    = (Mass_aer/Mass_inf)*100                               ! %
Ci_sor    = (Mass_sor/Mass_inf)*100                               ! %
Ci_bio    = (Mass_bio/Mass_inf)*100                               ! %
Ci_sum    = Ci_eff+Ci_was+Ci_vol+Ci_aer+Ci_sor+Ci_bio             ! %
```

! Effluent ENM Concentration
Ce=x1+(Kad*x1(a))*Xv_eff/1000**

```
!!!!!!!!!!!!!!!!!!!!!!!!!!!
! Write outputs to a file !
!!!!!!!!!!!!!!!!!!!!!!!!!!!
OPEN(unit=1, file='output.txt', status='replace')
WRITE(1,*) EQ_COD
WRITE(1,*) S_new
WRITE(1,*) UAP_new
WRITE(1,*) BAPS_new + BAPL_new
WRITE(1,*) COD_loading
WRITE(1,*) Rem_COD
WRITE(1,*) Xa_new
WRITE(1,*) Xres_new
WRITE(1,*) EPS_new
WRITE(1,*) BAPL_new
WRITE(1,*) XvSS
WRITE(1,*) Xv
```

```
WRITE(1,*) XSS
WRITE(1,*) X
WRITE(1,*) Xv/X
WRITE(1,*) thetah
WRITE(1,*) SWR
WRITE(1,*) O2uptake_kg
WRITE(1,*) FOTE_KK
WRITE(1,*) alpha_KK
WRITE(1,*) Power_KK
WRITE(1,*) Power_KK/Xg
WRITE(1,*) dXSS_dt
WRITE(1,*) O2input
WRITE(1,*) O2output
WRITE(1,*) O2uptake
WRITE(1,*) Qe_new
WRITE(1,*) Qw_new
WRITE(1,*) Ci
WRITE(1,*) Rem_Ci
WRITE(1,*) Mass_inf
WRITE(1,*) Mass_eff
WRITE(1,*) Mass_was
WRITE(1,*) Mass_vol
WRITE(1,*) Mass_aer
WRITE(1,*) Mass_sor
WRITE(1,*) Mass_bio
WRITE(1,*) Ci_eff
WRITE(1,*) Ci_was
WRITE(1,*) Ci_vol
WRITE(1,*) Ci_aer
WRITE(1,*) Ci_sor
WRITE(1,*) Ci_bio
WRITE(1,*) Ci_sum
CLOSE(1)



!!!!!!!!!!!!!!!!!!!!!!!!!!!!!!!!!!!!!!!!!!!!!!!!
! Might as well print it to the screen too !
!!!!!!!!!!!!!!!!!!!!!!!!!!!!!!!!!!!!!!!!!!!!!!!!
PRINT*,''
PRINT*,'EQ_COD = ',EQ_COD
PRINT*,'S_new = ',S_new
PRINT*,'Xa_new = ',Xa_new
PRINT*,'Xres_new = ',Xres_new
PRINT*,'EPS_new = ',EPS_new
```

```
PRINT*,'UAP_new = ',UAP_new
PRINT*,'BAPS_new = ',BAPS_new
PRINT*,'BAPL_new = ',BAPL_new
PRINT*,'COD_loading = ',COD_loading
PRINT*,'(COD_sum-EQ_COD)/COD_sum = ',(COD_sum-EQ_COD)/COD_sum
PRINT*,'COD_sum',COD_sum
PRINT*,'Rem_COD',Rem_COD
PRINT*,'XvSS = ',XvSS
PRINT*,'Xv = ',Xv
PRINT*,'XSS = ',XSS
PRINT*,'X = ',X
PRINT*,'Xv/X = ',Xv/X
PRINT*,'SWR = ',SWR
PRINT*,'O2uptake_kg = ',O2uptake_kg
PRINT*,'FOTE_KK = ',FOTE_KK
PRINT*,'alpha_KK = ',alpha_KK
PRINT*,'Power_KK = ',Power_KK
PRINT*,'Power_KK/Xg = ',Power_KK/Xg
PRINT*,'Qe_new = ',Qe_new
PRINT*,'Qw_new = ',Qw_new
PRINT*,'Xa_eff = ',Xa_eff
PRINT*,'Xa_rec = ',Xa_rec
PRINT*,'Ce liquid =',x1
PRINT*,'Ce = ',Ce
PRINT*,''


! Get total runtime
total_time = SECNDS(t0)
PRINT*,''
PRINT*,'Total time: ', total_time
PRINT*,''


END
```